LAWRENCE
LIVERMORE
NATIONAL
LABORATORY

UCRL-JRNL-217704

Boiling Temperature and Reversed Deliquescence Relative Humidity Measurements for Mineral Assemblages in the NaCl + NaNO3 + KNO3 + Ca(NO3)2 + H2O System

J. A. Rard, K. J. Staggs, S. D. Day, S. A. Carroll

December 13, 2005

Journal of Solution Chemistry

11/23/05

Boiling Temperature and Reversed Deliquescence Relative Humidity Measurements for Mineral Assemblages in the NaCl + $NaNO_3$ + KNO_3 + $Ca(NO_3)_2$ + H_2O System

Joseph A. Rard,[1,]* Kirk J. Staggs,[2] S. Dan Day,[2] and Susan A. Carroll[1]

Boiling temperature measurements have been made at ambient pressure for saturated ternary solutions of NaCl + KNO_3 + H_2O, $NaNO_3$ + KNO_3 + H_2O, and NaCl + $Ca(NO_3)_2$ + H_2O over the full composition range, along with those of the single salt systems. Boiling temperatures were also measured for the four component NaCl + $NaNO_3$ + KNO_3 + H_2O and five component NaCl + $NaNO_3$ + KNO_3 + $Ca(NO_3)_2$ + H_2O mixtures, where the solute mole fraction of $Ca(NO_3)_2$, $x\{Ca(NO_3)_2\}$, was varied between 0 and 0.25. The maximum boiling temperature found for the NaCl + KNO_3 + H_2O system is ≈134.9 °C; for the $NaNO_3$ + KNO_3 + H_2O system is ≈165.1 °C at $x(NaNO_3) \approx 0.46$ and $x(KNO_3) \approx 0.54$; and for the NaCl + $Ca(NO_3)_2$ + H_2O system is 164.7 ± 0.6 °C at $x\{NaCl\} \approx 0.25$ and $x\{Ca(NO_3)_2\} \approx 0.75$. The NaCl + $NaNO_3$ + KNO_3 + $Ca(NO_3)_2$ + H_2O system forms molten salts below their maximum boiling temperatures, and the temperatures corresponding to the cessation of boiling (dry out temperatures) of these liquid mixtures were determined. These dry out temperatures range from ≈300 °C when $x\{Ca(NO_3)_2\} = 0$ to ≥ 400 °C when $x\{Ca(NO_3)_2\} = 0.20$ and 0.25. Mutual deliquescence/efflorescence relative humidity (MDRH/MERH) measurements were also made for the $NaNO_3$ + KNO_3 and NaCl + $NaNO_3$ + KNO_3 salt mixture from 120 to 180 °C at ambient pressure. The $NaNO_3$ + KNO_3 salt mixture has a MDRH of 26.4% at 120 °C and 20.0% at 150 °C. This salt mixture also absorbs water at 180 °C, which is higher than expected from the boiling temperature experiments. The NaCl + $NaNO_3$ + KNO_3 salt mixture was found to have a MDRH of 25.9% at 120 °C and 10.5% at 180 °C. The investigated mixture compositions correspond to some of the major mineral assemblages that are predicted to control brine composition due to the deliquescence of salts formed in dust deposited on waste canisters in the proposed nuclear repository at Yucca Mountain, Nevada.

KEY WORDS: Boiling temperature; deliquescence relative humidity; efflorescence relative humidity; saturated solutions; sodium chloride; sodium nitrate; potassium nitrate; calcium nitrate; aqueous solutions.

[1] Energy and Environmental Directorate, University of California, Lawrence Livermore National Laboratory Livermore, California 94550.
[2] Chemistry and Materials Science Directorate, University of California, Lawrence Livermore National Laboratory, Livermore, California 94550.
* Corresponding author; email: rard1@llnl.gov.

1. INTRODUCTION

Yucca Mountain, Nevada is the designated site for a geologic repository for the permanent disposal of high-level nuclear waste. The current waste package design uses double walled waste containers with an inner wall of stainless steel and an outer wall of highly corrosion resistant Ni-Cr-Mo alloy that contains lesser amounts of W and Fe ("Alloy 22"), which are protected with Ti-Pd alloy drip shields to prevent falling rocks and seepage water from coming into direct contact with the containers.[1] The corrosion resistance and long-term integrity of these metal barriers directly affect the performance of this design. If the Yucca Mountain site license is approved, then the waste packages will be emplaced in tunnels several hundred meters below the ground surface in partially saturated volcanic tuff, but will still be well above the groundwater table. Concentrated brines could form on the waste packages by deliquescence of hygroscopic salts found in local and regional dust deposited during repository construction, and from dust brought in by ventilation.

The accurate prediction of the conditions in which brines form is important for the safe disposal of radioactive waste, because brine composition will directly affect the corrosiveness of these solutions to the waste canister, and the relationship between deliquescence relative humidity and temperature is an indicator of "repository dryness". The range of brine compositions formed by the deliquescence of hygroscopic salts found in these dusts can, in principle, be calculated using equilibrium thermodynamics, because the relative humidity is directly related to the activity of water and thus to the solution composition. If the salts in this tunnel dust deliquesce, the resulting hot concentrated salt solutions could potentially initiate corrosion of the metal waste containers and drip shields. Whether this happens will depend mainly on the temperature, pH, and chemical

composition and concentration of the solutions formed when this deliquescence occurs, and whether the thus formed solution droplets are in direct contact with the surface of the waste package. It is therefore of critical importance to know whether multicomponent brines can form at elevated temperatures by deliquescence of salts present in the repository tunnel dust, their chemical composition, and in what relative humidity and temperatures ranges these brines can persist. This information is especially needed above 120 °C, which is the estimated upper temperature limit of applicability for the current corrosion model being used.[2]

The relative and absolute concentrations of the anions Cl^- and NO_3^- will have a major impact on the corrosive ability of these brines; higher NO_3^- to Cl^- ratios reduce the likelihood of crevice corrosion of Alloy 22 by acidic chloride solutions at least at lower and intermediate ionic strengths.[3] High nitrate ion concentrations have been observed in solutions formed from the evaporative concentration of groundwater whose initial nitrate concentration is low.[4,5] Thermodynamic modeling of the deliquescence behavior of the soluble salts leached from dust collected at the Yucca Mountain Repository Site, using EQ3/6 simulations of the evaporation sequence (but not including the effect of ammonium ions present in atmospheric aerosols), indicates that the following three salt assemblages are most important for controlling deliquescence. Assemblage A consists of the $NaCl + KNO_3 + H_2O$ system, Assemblage B the $NaCl + NaNO_3 + KNO_3 + H_2O$ system, and Assemblage C the $NaCl + NaNO_3 + KNO_3 + Ca(NO_3)_2 + H_2O$ system.[1] The presence of these nitrate salts can considerably reduce the relative humidity at which deliquescence of salt mixtures occurs at high temperatures, as a consequence of their considerable solubility at elevated temperatures.[6,7]

Reverse deliquescence experiments were reported for the $NaNO_3 + KNO_3 + H_2O$ system at 90 to 120 °C.[8,9] The measured deliquescence relative humidity (DRH) results agree fairly well with predictions made using the EQ3/6 geochemical modeling code[10] for mixtures with $NaNO_3$ molality fractions $x(NaNO_3) > 0.4$, but there are significant discrepancies for solutions with $x(KNO_3) > 0.6$. These x values are the solute mole fractions (the amount of water is not included when calculating these mole fractions). The predicted molalities of the solutions in the vicinity of the eutonic composition are lower than the experimental values by up to a factor of two.

These significant errors in the model predictions occur because of deficiencies in the Pitzer ion-interaction model[11] parameter thermodynamic database used in these calculations.[10] Although the Pitzer ion-interaction model parameters for most of the single salts are available over wide ranges of temperature, those for KNO_3(aq) and the $\theta(Cl,NO_3)$ mixing parameter are only available at 25 °C and were thus assumed to be independent of temperature for the high temperature modeling calculations. These approximations are expected to give increasingly more serious prediction errors as the temperature is increased because the saturated solution molalities of these solutions increase very rapidly with increasing temperature. Furthermore, modeling calculations for solutions containing $Ca(NO_3)_2$ do not converge at temperatures much above 60 °C. At and above 60 °C the ratio of the number of water molecules per ion in a saturated $Ca(NO_3)_2$ solution drops below one, as do the ratios of water molecules per ion in $NaNO_3$(aq) and KNO_3(aq) solutions at elevated temperature.[6,7] Such high concentrations are quite outside the intended range of validity of Pitzer's model and all other thermodynamic models based on the molality composition scale.

Temperature-dependent KNO_3(aq) binary solution Pitzer parameters and mixing parameter values valid to high temperatures are needed for improving the thermodynamic modeling predictions, as are other parameterized thermodynamic models valid to extremely high concentrations, but are not yet available. Consequently, in order to understand the behavior of the three mineral assemblages at high temperatures, we measured boiling temperatures for Assemblages A, B, and C, NaCl + KNO_3 + H_2O, NaCl + $NaNO_3$ + KNO_3 + H_2O, and NaCl + $NaNO_3$ + KNO_3 + $Ca(NO_3)_2$ + H_2O, respectively, along with their subsystems $NaNO_3$ + KNO_3 + H_2O and NaCl + $Ca(NO_3)_2$ + H_2O. These measurements directly establish the upper temperature limits at which deliquescence can occur in these salt mixtures, and will provide guides for future geochemical modeling calculations. In addition, mutual deliquescence/efflorescence relative humidity (MDRH/MERH) measurements were made for $NaNO_3$ + KNO_3 and NaCl + $NaNO_3$ + KNO_3 salt mixtures from 120 to 180 °C, which supplement previous reported measurements at lower temperatures[8,9] and which provide direct information about deliquescence conditions below the saturated solution boiling temperatures.

2. EXPERIMENTAL DESCRIPTION

The boiling temperature measurements and the experimental results are described in more detail in preliminary reports.[12,13]

2.1. Boiling Temperature Measurements

2.1.1. The Boiling Temperature Apparatus and the Temperature Measurements

The measurements were made using an apparatus constructed from a 1 L flat bottom pyrex kettle to which an upper pyrex glass section was clamped firmly in place. The upper section has four standard taper openings on the top. The largest (central) opening was

fitted with a water-cooled condenser column to control the amount of water evaporation during the experiments. The shaft of a three-blade propeller stirrer (Teflon coated) was inserted into the solution region of the apparatus through the center of the condenser column, which allowed the solution to be rapidly mixed to reduce the formation of concentration and temperature gradients as the solution was heated and the solubility changes. The other three ports are located at 120° intervals towards the edge of the top of the upper section. All three of these outer ports were normally closed with rubber stoppers during the boiling temperature measurements. One port was opened when dry salts or water were added to this vessel using a plastic funnel, for the visual observation of the boiling of the solution, and when solutions were being concentrated by evaporation of solvent, but otherwise it was closed. The other two ports were used for thermocouple probes, which were inserted through the centers of the rubber stoppers. The internal volume of the boiling temperature apparatus is approximately 1 L, of which typically about 200 to 400 mL was occupied by solution and solid during the boiling temperature measurements. The bottom section of the apparatus is surrounded by a heating mantle, with heat being applied separately to the bottom and to the sides of the apparatus (the heating mantle extends above the solution level). A schematic of this apparatus is shown in Fig. 1.

Except for a few of the earliest experiments where only a single thermocouple probe was used, two thermocouple probes were present in the solutions during the boiling temperature measurements. The first thermocouple probe was positioned in the solution near the edge of the flask and outside the sweep of the propellers of the stirrer. The second thermocouple probe was inserted into the solution near the center of the flask and above the sweep of the propellers of the stirrer. Type T thermocouples coated with Teflon were used in the majority of the experiments. However, the temperatures encountered for the NaCl +

$NaNO_3 + KNO_3 + Ca(NO_3)_2 + H_2O$ system generally exceed 300 °C, and the Teflon coating of the thermocouples melted off during an experiment when the temperature exceeded 350 °C. These two thermocouples were replaced by Type T thermocouples contained in uncoated inconel wells for the remaining $NaCl + NaNO_3 + KNO_3 + Ca(NO_3)_2 + H_2O$ experiments. All four thermocouples were calibrated (with standards traceable to NIST) by Heusser Neweigh before and by Bechtel Nevada after the boiling temperature measurements were made. Calibrations done at approximately 0, 100, and 200 °C for the first pair of thermocouples after they were stripped of their Teflon coating agreed with their previous calibration values to within 0.1 °C, which is within the uncertainty of the calibration; this indicates that they were undamaged when the Teflon coating melted. One of these thermocouples was used above its calibrated range for three measurements in the 297 to 354 °C temperature range.[13] An in-house calibration was made for this thermcouple using an Omega hot-point cell. The calibration results agreed with the nominal results in the 250 to 395°C temperature region to within 0.53 to 0.69 °C, which is within the ±0.7 °C uncertainty of these temperature calibration measurements.

The thermocouples were interfaced either with a Beamex Multifunctional Calibrator or an ΩEOMEGA 450ATT Hand Held Reader. The upper temperature limit for the ΩEOMEGA Hand Held Reader is 204 °C whereas for the Beamex Multifunctional Calibrator it is 400 °C; above these temperatures the temperature readers go off scale.

The temperature readings from the second thermocouple probe, which is located near the center of the boiling temperature apparatus, were found to be less affected by the temperature gradient between the heating mantle and the solution being investigated. Thus the corrected temperatures reported in Tables I through V are generally based on the readings of this second probe.

Numerous determinations were made of the boiling temperature of water at ambient pressure. Examination of the critically assessed vapor pressures of water in the Handbook of Chemistry and Physics[14] at the recorded pressures allowed the true boiling temperatures to be determined that correspond to the recorded pressures, and these values were compared with the measured boiling temperatures of water. The observed boiling temperatures were always slightly higher (≈ 1 °C) than the correct values, implying that there is a small effect from heat transport rate limitations even near the center our boiling temperature apparatus. Accordingly, the nominal boiling temperatures were adjusted downward to yield complete agreement for the boiling temperatures of water measured with the second (inner) thermocouple.

Based on the size of the temperature corrections (≈ 1 °C), the reproducibility of the measured boiling temperatures for pure H_2O and saturated aqueous solutions of the single salts (Table I), and agreement of the boiling temperatures of saturated single salt solutions with literature values,[15] the uncertainties in the reported corrected temperatures are estimated to be about 0.5 °C for temperatures around 100 °C and about 1 °C for temperatures around 200 °C. For temperatures much above 200 °C to about 300 °C the uncertainties are around 2 °C. For the $NaCl + NaNO_3 + KNO_3 + Ca(NO_3)_2$ system with $x\{Ca(NO_3)_2\} \geq 0.05$, the uncertainties of the dry out temperatures are somewhat larger because of difficulty in observing when boiling ceases.

For most experiments, Teflon boiling chips and/or glass beads were added to the solutions in the apparatus to prevent possible slight superheating. Teflon melts around 350 °C and thus only glass beads were used at temperatures above 350 °C.

No in-laboratory calibrated pressure measuring system was available for these experiments, and the reported pressure for each experiment is the atmospheric pressure at

the Lawrence Livermore National Laboratory (LLNL) site at the time closest to that of a boiling temperature measurement, as reported by the LLNL weather station internet web site (http://www-met.llnl.gov).

2.1.2. Source Chemicals and Preparation of the Solutions

The mixtures used for the boiling temperature experiments were prepared by weight using the solid salts and purified water. The source NaCl, $NaNO_3$, and $Ca(NO_3)_2{\cdot}4H_2O$ chemicals used for all of the experiments were supplied by J. T. Baker ("Baker Analyzed"). J. T. Baker KNO_3 was used in some of the boiling temperature experiments whereas Merck KNO_3 was used in others.

The salt samples were weighed to a precision of 1×10^{-4} g using a Sartorius MC 210S balance, with daily checks on the accuracy using standard weights. Based on the weighing uncertainties and calibrations, all sample weights should be reliable to ≤ 0.01 %. All water used in the experiments was purified using a Barnstead E-Pure water treatment system.

No attempt was made to dry the chemicals used for the experiments with two exceptions. The Merck KNO_3 was coarser grained than the J. T. Baker KNO_3, and the Merck sample showed a slow weight loss for several hours after being removed from the storage container. It was thereafter allowed to equilibrate with the laboratory atmosphere for overnight or longer, which eliminated this problem (presumably the result of drying of small amounts water present in the source chemical). The J. T. Baker $Ca(NO_3)_2{\cdot}4H_2O$ showed similar slow weight changes when removed from the original bottle, presumably indicating the initial presence of a water content slightly greater that of the thermodynamically stable hydrate at this temperature.

The purities of most of the lots of J. T. Baker NaCl, $NaNO_3$, and KNO_3 used were given by the supplier as 99.9 %, with all falling in the range 100.0 ± 0.2%. Based on the cation and anion impurity analysis results reported by the supplier, other anions and cations that were present were in insignificant amounts, and it is likely that most of the reported 0.1% to 0.2% impurities are actually residual water. Dehydration experiments[16] for two commercials samples of NaCl(s) showed the presence of 0.1 to 0.15 mass-% residual water in the original samples, which was not completely removed until the NaCl samples were heated to ≈500 °C. The effect of the presence of this residual water largely cancels out when solute mole fractions are calculated. Samples of $Ca(NO_3)_2{\cdot}4H_2O$ from two different lots were used in the experiments, with reported lot analyses of 99.6 and 102.1 %. Because the total amounts of identified elemental impurities did not exceed 0.01 %, the deviations from 100 % $Ca(NO_3)_2{\cdot}4H_2O$ stoichiometry are presumably due to a deficiency or excess of water. The water activity of a saturated solution in equilibrium with $Ca(NO_3)_2{\cdot}4H_2O$ at 25 °C is $a_w = 0.500$,[17] and because the relative humidity in our laboratory is typically around this value, the composition of the air-dried samples used in the experiments was presumed to be stoichiometric $Ca(NO_3)_2{\cdot}4H_2O$.

The number of moles of each salt were calculated from the apparent sample masses (*i.e.*, without buoyancy corrections) assuming that the molar masses are 58.443 g-mol^{-1} for NaCl, 84.99 g-mol^{-1} for $NaNO_3$, 101.11 g-mol^{-1} for KNO_3, and 236.15 g-mol^{-1} for $Ca(NO_3)_2{\cdot}4H_2O$. In principle, the calculation of the number of moles should be based on sample masses rather than the apparent masses. However, buoyancy corrections were not required because their effects will almost completely cancel when solute mole fractions are calculated.

Based on the uncertainties and weighing errors described in the preceding three paragraphs, the solute mole fractions reported in this paper, which were calculated from the amount of added salt, should be accurate to ≤ 0.2 %.

2.1.3. Basic Procedure for the Determination of Boiling Temperatures of Saturated Solutions

The basic experimental procedure is as follows. Approximately 100 to 150 mL of purified water (the exact amount is not important) was added to the boiling temperature apparatus. Sample of one or more of the salts were separately weighed using individual plastic weighing boats, and the weighed solid(s) was (were) transferred to the boiling temperature apparatus through an open port. The heaters in the heating mantle were turned on and heating was continued until the solution began boiling (and was concentrated sufficiently, if necessary, until solid phase was present), and then the boiling temperature of the saturated solution was recorded along with the ambient pressure. However, $Ca(NO_3)_2{\cdot}4H_2O$(cr) melts in its own water of hydration, and solutions containing it were evaporated until a solid phase was produced.

The amount of salt present in their saturated solutions of the investigated mixtures at their boiling temperatures is quite high, and it increases very rapidly with increasing temperature. Attempts to sample the solution phase were fraught with difficulties, because the slight cooling that occurred during sample removal resulted in large amounts of precipitation that clogged up the syringe and filters required to remove the samples and filter out solid material suspended in these viscous solutions. This precipitation should also cause the ratio of salts present in the solution phase to change from that present in the boiling solutions. Consequently, the reported mole fractions were calculated from the mass of each added salt. However, because of the presence of unknown amounts of one or more

solid salts in these saturated solution experiments, the molar ratios of salts present in some of the solution phases may differ significantly from the ratios calculated from the masses of salts added to the system. This lack of information about the relative amounts of each salt in the solution phase gives rise to the observed scatter in some of the plots of boiling temperatures *versus* mole fraction composition

2.1.4. Melting Temperature Determinations

Melting/solidification temperatures were measured with differential scanning calorimetry (DSC) using a TA Instruments DSC 2910. The measurements were made using a sample of the first mixture reported in Table V, NaCl + $NaNO_3$ + KNO_3 with $x\{NaCl\}$ = 0.32002, $x\{NaNO_3\}$ = 0.31299, and $x\{KNO_3\}$ = 0.36699. A sample of the anhydrous mixture was removed while molten and then allowed to solidify before being used for the DSC measurements. An additional sample having essentially the same salt mole fractions was prepared by direct weighing of the anhydrous salts, followed by repeated mixing and grinding to produce a more nearly homogeneous sample. In addition, melting/solidification temperatures were measured for the source $NaNO_3$ and KNO_3 samples.

Temperatures determined on the heating and cooling cycles of the DSC measurements showed some difference from kinetic factors related to thermal conductivity, with the temperatures obtained during the cooling cycle being higher. Comparison of the measured melting temperatures of $NaNO_3$(cr) and KNO_3(cr) to literature values[7,14] indicated that those obtained on the cooling cycle are more accurate due to a smaller thermal lag. The melting temperatures thus determined for the two NaCl + $NaNO_3$ + KNO_3 samples were in good agreement yielding an average of 218 ± 3 °C. This value is very slightly lower than the minimum melting/freezing temperatures of 220 to 223 °C reported for the $NaNO_3$ + KNO_3 system.[15] The presence of NaCl apparently had a minimal effect

on the minimum melting/freezing temperatures of the NaCl + $NaNO_3$ + KNO_3 system. We note that a lower intensity peak, which corresponds to the rhombohedal to trigonal phase transition that occurs in pure phase KNO_3(cr) around 129 °C,[14] was also observed in the NaCl + $NaNO_3$ + KNO_3 sample recovered from the dry out temperature experiment, indicating the present of some excess KNO_3 in the solid phase.

2.2. Deliquescence/Efflorescence Relative Humidity Measurements

2.2.1. The Resistivity Cell and its Operation

We also measured the mutual deliquescence (MDRH) and efflorescence (MERH) relative humidities of KNO_3 + $NaNO_3$ and NaCl + KNO_3 + $NaNO_3$ salt mixtures from 120 to 180 °C by varying the relative humidity and monitoring the resistivity changes of the salt systems. The basic premise behind the resistivity experiments is that the resistance will significantly drop at the MDRH for a given salt mixture as brine solution forms by deliquescence of the solid mixtures. Likewise, efflorescence will correspond to a significant increase in resistance as the brine solution dries out to from the solid salt mixture. This basic approach was used previously by Pabalan and co-workers[18,19] to measure the DRH of pure salts and NaCl + KNO_3 salt mixtures at lower temperatures.

All mutual deliquescence/efflorescence relative humidity experiments were conducted in Ecosphere/Despatch environmental chambers to control both temperature and relative humidity. The maximum temperature was limited to 180 °C to prevent deterioration of the relative humidity probe that would occur at higher operating temperatures. The upper limit of the relative humidity for our apparatus at each temperature was limited by the vapor pressure of water at the ambient atmospheric pressures. Pre- and post-experiment calibrations of the relative humidity probes were

made using the bi-thermal apparatus described below. The reported uncertainty is calculated as the standard deviation of the pre and post-calibration RH values.

The resistivity was measured using two parallel platinum electrodes, separated by less than 1 mm, set in a recessed resistivity cell made of PPS (polyphenylene sulfide), which is stable to above 180 °C. The length of the electrodes exposed to the solution was about 2.5 cm. Comparison of experiments conducted with a quartz slide as an inert surface with those made with the PPS cell suggests that PPS is inert to the investigated brines, with no significant sorption of water at the investigated low relative humidities and high temperatures.[20] The resistance was monitored with an automated data acquisition system using a Gamry PCI4/300 Potentiostat, in which one Pt-electrode was the working electrode and the other was the counter and reference electrode. All measurements were recorded in the electrochemical impedance spectroscopy (EIS) mode at 5 kHz, where the voltage reference and the direct current voltage bias were set to zero, with an alternating current voltage of 20 or 25 mV. The temperature and relative humidity inside the environmental chamber were measured right above the sample cells during the course of the resistivity measurements. A schematic of the resistivity cell is shown in Fig. 2.

All experiments were done with enough dissolved salt initially present to provide a conductive path between the electrodes (about 80% coverage). The temperature was then increased to the selected temperature, and the relative humidity was lowered to achieve complete dry out of the salt solution, which was marked by a high impedance reading. The relative humidity was then increased in 2% RH increments, and held there for six hours to avoid recording intermediate events. The relative humidity was incrementally increased until several percentage units beyond the mutual deliquescence

relative humidity value, which is marked by a sharp reduction in resistivity. The process is then reversed with incremental decreases in the relative humidity, in order to measure the mutual efflorescence relative humidity. After a series of measurement was finished for a particular mixture composition, the cells were cleaned and the impedance checked before a new solution was added.

2.2.2. Calibration of the Relative Humidity Probes using a Bi-thermal Apparatus

In 1947 Stokes[20] described the use of an apparatus for determining the vapor pressures of aqueous solutions, in which a solution of an electrolyte was maintained at a higher temperature (T_h) and pure water was maintained at a lower temperature (T_l). In this apparatus the water vapor was allowed to diffuse through an interconnected vapor phase until the solution gained or lost enough water so that its vapor pressure became equal to that of pure water at temperature T_l. Because the vapor pressure of pure water is accurately known as a function of temperature, by knowing the temperature of the lower temperature water reservoir (T_l), the vapor pressure $p_w(T_h)$ of the higher temperature solution is also known. After equilibrium was reached, the solution was removed and analyzed to determine its molality m. This experiment yielded a determination of m and $p_w(T_h)$, from which the water activity a_w at T_l could be calculated. Stokes referred to this method as bi-thermal equilibrium through the vapor phase.

Consider the alternative situation where the lower temperature reservoir contains some pure liquid water at temperature T_l where the saturation water vapor pressure at this temperature is $p_w^o(T_l)$, and the higher temperature reservoir contains only a vapor phase (no liquid water or solution is present) and is kept at temperature T_h. After vapor diffusion of water between the two reservoirs has occurred for a sufficiently long time, bi-thermal equilibrium is reached where the water vapor pressure will be the same in the two

reservoirs. However, the water vapor pressure in the higher temperature reservoir $p_w(T_h)$ will be below saturation at that temperature. At equilibrium,

$$p_w(T_h) = p_w^o(T_l) \tag{1}$$

The relative humidity occurring in the lower temperature reservoir will always be 100 % at the liquid water/water vapor interface. In the higher temperature compartment the relative humidity is given by

$$\begin{aligned} \mathrm{RH} &= 100\{p_w(T_h)/\, p_w^o(T_h)\} \\ &= 100\{\, p_w^o(T_l)/\, p_w^o(T_h)\} \end{aligned} \tag{2}$$

Thus the relative humidity in the higher temperature compartment is determined uniquely by the ratio of the saturation vapor pressures of pure water at the two temperatures T_h and T_l.

The rate at which the vapor pressure of water reaches equilibrium between the higher and lower temperature reservoirs depends on the size of the reservoirs and the length and cross-sectional area of the path connecting the two reservoirs. The time to reach bi-thermal equilibrium needs to be determined by monitoring the RH in the high temperature reservoir as a function of time, until a steady state value is obtained. We found that when the temperature of the lower temperature reservoir was below 100 °C, the rate of transport of water vapor was too slow to yield a steady state in a reasonable period of time. Consequently, all calibrations of relative humidity probes with the apparatus were made with the lower temperature reservoir set at the boiling temperature of water.

The bi-thermal high temperature RH probe calibration system was assembled using two multi-port 1000 mL glass flasks, each housed in separate convection ovens, and connected with a combination of glass and Teflon™ fittings and piping as shown in Fig. 3. The temperatures inside the two ovens (VWR model 1330FZZ) were controlled and monitored throughout the measurements using a computer based data acquisition system consisting of the following components: Dell Optiplex GS260 (Window 2000 Professional operating system), data acquisition software: DasyLabs version 7.00.05 (DASYTec USA), IOtech DaqBook model 2000A, IOtech DBK84 Thermocouple Module, IOtech DBK42 5B Signal Conditioning Chassis, IOtech 5B RTD modules model SCM5B34-03, and IOtech DBK5 4 channel current output card. Critical temperature measurements, required to determine the RH at elevated temperatures, were made using a high precision thermometer and probe (NIST traceable calibration), with a temperature resolution of 0.001 °C and an accuracy of 0.07 °C.

One of the flasks was used as the system steam generator (saturator) and the other as the high temperature reservoir (non-condensing vessel) for the RH probe calibrations. In preparation for and during its operation, the saturator was approximately half full with deionized water, and was heated in the convection oven whose temperature was set between 150 and 160 °C. The water in the flask, which was boiling, was of course at 100 °C. This furnace temperature range was selected to ensure that the water within the saturator was maintained at its boiling point through the experiments.

The interconnecting tube and fittings connecting the two ovens were wrapped with heat tape and heated to 160 °C using a temperature controller; this prevents condensates from forming in these components. The valve located in the middle of the

interconnecting tube was used while purging the system of air, and as a pressure tap to monitor pressure within the system during periodic checks or evaluations of system performance.

Soft silicone stoppers were used to seal around twisted and irregular probe cables and tubes in both vessels. This type of seal was selected because it can withstand the high temperatures and easily conforms to the irregular shapes of the cables connecting the probes to the RH meter. Although some outward leakage of air and steam occurs around the cables, it provided an adequate path to purge the system of dry air and replace it with saturated steam during operations and ensured that a water vapor saturated atmosphere was maintained through the system. During measurements the system pressure was consistently measured using between 2.5 and 7.5 cm of head in a liquid water-filled manometer relative to ambient vapor pressure.

The oven containing the non-condensing vessel was controlled through the computer based data acquisition system and heated to selected temperatures that were measured at the center of the non-condensing vessel. To prepare the system for measurements, all probes to be tested and the high-precision thermometer probe (with NIST traceable calibration) were inserted into the non-condensing vessel with the sensing element of each probe at mid level in the vessel. Since the wall of the test vessel was slightly hotter than the air temperature inside the vessel, care was taken to ensure that the sensor did not touch the wall of the vessel.

The interconnecting tube heaters and the non-condensing test vessel were heated prior to heating the saturator. With the humidity and temperature probes in place, the oven containing the non-condensing test vessel was turned on and the probes and

surrounding vessel air were allowed to heat to the selected temperature until the temperature readings became stable (typically 2 to 4 hours). With both the interconnecting tube and non-condensing vessel at their set temperatures, the saturator was heated until reaching its temperature and the RH stabilized (typically 1 to 2 hours) in the non-condensing vessel. At each set point, three readings of the non-condensing vessel air temperature and RH probe readings were manually recorded and averaged. This process was repeated at a least four different temperature settings spanning the selected temperature range.

Because temperature gradients are present within the non-condensing test vessel, the temperature probe of the RH meter provides a more accurate means of determining the value of $p_{\mathrm{w}}^{\mathrm{o}}(T_{\mathrm{h}})$ and thus RH at the RH probe sensor. As a requirement, prior to using the RH meter temperature probe, its was calibrated against the NIST traceable high precision thermometer.

Table VI gives values of the RH calculated at selected temperatures for the higher reservoir with the lower temperature reservoir fixed at 100.00 °C, based on values of vapor pressure of water ("steam tables") reported in the Handbook of Chemistry and Physics.[14] Figure 4 shows the results of several calibrations of our relative humidity sensor probe. The response of this probe is compared with the standard values calculated from the steam tables at the experimental temperatures. The least-squares fits of relative humidity (standard) *versus* relative humidity (measured) have correlation coefficients R > 0.999, indicating a linear relationship. The variation from calibration-to-calibration as indicated by changes in the intercepts (see inserts in Fig. 4), are ≤ 1.2 % RH units. The uncertainty in the measured RHs is estimated from the standard deviations calculated

separately from the pre-experimental and post-experimental calibrations, are typically less than 1.5 % RH units.

3. RESULTS

3.1. Boiling Temperatures

3.1.1. Binary Solutions

Timmermans[15] lists values of the "normal boiling points" of saturated aqueous solutions of various salts, mainly from measurements made in the 1880s and early 1900s when the temperature scales were not as well defined. Boiling temperatures listed by Timmermans for saturated NaCl + H_2O solutions are 108.50, 108.668, and 109 °C; for $NaNO_3$ + H_2O are 120.20, 121, and 122 °C; for KNO_3 + H_2O are 115.549, 115.9, and 118 °C; and for $Ca(NO_3)_2$ + H_2O is 152 °C. Ewing[21] reported a similar value of 151 °C for $Ca(NO_3)_2$ + H_2O. The last value for saturated KNO_3 + H_2O (published in 1856) is presumably an outlier. After taking into account that our experimental pressures reported in Table I are slightly lower than 1 atmosphere (= 1.01325 bar), our boiling temperatures are in good agreement with those listed by Timmermans.[15]

3.1.2. NaCl + KNO_3 + H_2O and $NaNO_3$ + KNO_3 + H_2O Solutions

Boiling temperatures for the saturated NaCl + KNO_3 + H_2O and $NaNO_3$ + KNO_3 + H_2O systems were measured over the full composition range. The plots of boiling temperature against solute mole fraction compositions are based on use of the mole fraction as calculated from the masses of each solute added to the mixtures.

Based on the plot of boiling temperature *versus* the "as added" solute mole fraction composition, Fig. 5.a, we estimate that the maximum boiling temperature composition for saturated solutions in the NaCl + KNO_3 + H_2O system occurs at x(NaCl) ≈ 0.32 and

$x(KNO_3) \approx 0.68$ with a maximum boiling temperature of 133.8 °C. A direct determination of this maximum boiling temperature was made by evaporating a boiling saturated solution with an initial composition $x(NaCl) \approx 0.5001$ and $x(KNO_3) \approx 0.4999$ until the boiling temperature no longer increased. The directly measured value of 134.9 °C at $p = 0.996$ bar (given in Table I), with an uncertainty between 0.5 and 1.0 °C, is in very good agreement with the estimated value from the plot.

Solubility data summarized by Linke[7] indicate that the maximum boiling temperature should occur at $x(NaCl) \approx 0.14$ and $x(KNO_3) \approx 0.86$, rather than $x(NaCl) \approx 0.32$ and $x(KNO_3) \approx 0.68$ as implied by Fig. 5.a. Thermodynamic modeling calculations by T. J. Wolery (private communication) indicate that at our investigated temperatures and concentrations sylvite (KCl) should precipitate from the concentrated $NaCl + KNO_3 + H_2O$ solutions, causing the solution composition to differ significantly from that for a simple $NaCl + KNO_3$ mixture. That is, the solutions must be considered as being mixtures where the sum of the ionic molalities are equal, $m(Na^+) + m(K^+) = m(Cl^-) + m(NO_3^-)$, but $m(Na^+) \neq m(Cl^-)$ and $m(K^+) \neq m(NO_3^-)$. The scatter in boiling temperatures shown in Fig. 5.a is probably the result of different (and unknown) amounts of precipitation of sylvite, which have been observed to form in these mxtures.[9] This precipitation results in changes in the relative amounts of salts present in the solution phase, which cannot be accommodated on this plot. Because of the uncertainty in solution compositions, our presentation of the boiling temperatures is limited to Fig. 5.a and the numerical results are not reported. However, we note that in spite of these uncertainties, Fig. 5.a still yielded a reliable estimate of the maximum boiling temperature for saturated solutions in the $NaCl + KNO_3 + H_2O$ system.

The measured boiling temperatures for saturated solutions in the $NaNO_3 + KNO_3 + H_2O$ system are summarized in Table II. Similarly, from a plot of boiling temperature *versus* solute mole fraction composition for saturated solutions in this system, Fig. 5.b, we estimate that the maximum boiling temperature composition for saturated solutions will occur at $x(NaNO_3) \approx 0.46$ and $x(KNO_3) \approx 0.54$ with a maximum boiling temperature of roughly 160 °C. A direct determination of this temperature was made by evaporating a boiling saturated solution with an initial composition $x(NaNO_3) \approx 0.5001$ and $x(KNO_3) \approx 0.4999$ until the temperature no longer increased. The directly measured value of 165.1 °C at $p = 1.005$ bar (given in Table II), with an uncertainty between 0.5 and 1.0 °C, is in satisfactory agreement with the estimated value but is higher. The major uncertainty in the ≈ 160 °C estimate arises because it was based on a plot of boiling temperature *versus* the "as added" composition, rather than the true solution composition that is unknown. We note that changes in slope occur in both the right-hand ($NaNO_3$ rich) and left-hand (KNO_3 rich) sections of Fig. 5.b at temperatures around 130 to 135 °C. These slope changes are presumably a reflection of the rhombohedal to trigonal phase transition that occurs in pure phase KNO_3(cr) around 129 °C.[14]

Some of the experiments involved separate boiling temperature measurements using the same mixtures of $NaNO_3 + KNO_3$, but were made on separate days. The first boiling temperature determined for each of these compositions was measured after the fresh addition of one or more of the component salts. After these initial boiling temperatures were measured, the heater was turned off after normal working hours, and the solutions cooled down. After cooling to room temperature, little or no liquid phase remained and the samples were mostly or entirely solid. The solid residue was reheated with addition of small amounts of water to produce the solution used for the second boiling temperature

determination. In the second boiling temperature determinations and subsequent ones, the solid phase consisted of some of the undissolved residue remaining from the previous experiment, and the observed boiling temperature was always higher for the later determinations.

When these very concentrated hot solutions were allowed to cool, the resulting solid phase was white, glassy in appearance, very hard, and somewhat slow to dissolve in water. According to the information given by Linke,[7] below 105 °C both solid $NaNO_3$ and KNO_3 are stable as pure phases in contact with saturated $NaNO_3 + KNO_3 + H_2O$ solutions, depending on the salt ratio, but above 150 °C they form a continuous series of solid solutions. The observed shift to higher boiling temperatures for the repeat boiling temperature determinations must result from changes in the composition of the solution and/or its co-existing solid phase, which could be due to the formation of a solid solution or because of changes in the solution phase solute ratios as it evolves towards the maximum boiling temperature composition.

The possible solid phases in the $NaNO_3 + KNO_3 + H_2O$ system are $NaNO_3$, KNO_3, and their solid solutions. The observed maximum boiling temperature of 165.1°C is ≈ 45 °C above that for the limiting binary solution $NaNO_3 + H_2O$ and ≈ 50 °C above that for the other limiting binary solution $KNO_3 + H_2O$. Available solubilities[7] for the $NaNO_3 + KNO_3 + H_2O$ system yield maximum boiling temperature compositions (assumed to correspond to those of the eutonic composition at each temperature) of $x(NaNO_3) = 0.391$ at 125 °C, $x(NaNO_3) = 0.425$ at 150 °C, and $x(NaNO_3) = 0.467$ at 175 °C. Graphical interpolation of these values yield an estimated mole fraction of $x(NaNO_3) \approx 0.45_3$ at our maximum boiling temperature of 165.1 °C, which agrees fairly well with the value of $x(NaNO_3) \approx 0.46$ estimated from the plot of our boiling temperatures *versus* $x(NaNO_3)$. The

solubility data tabulated by Linke yield total molalities m_T (which is equal to the ionic strength because both electrolytes have the same charge type) for $NaNO_3 + KNO_3$ of m_T = 70.6 mol·kg^{-1} at 125 °C, m_T = 95.5 mol·kg^{-1} at 150 °C, and m_T = 160 mol·kg^{-1} at 175 °C. Graphical interpolation of these results yields an estimate of the molality / ionic strength of the eutonic composition, $m_T \approx 130$ mol·kg^{-1}, at the maximum boiling temperature of 165.1 °C. These saturated solution molalities are considerably higher than those observed for the single salt systems $NaNO_3 + H_2O$ and $KNO_3 + H_2O$ at these temperatures.[7]

3.1.3. $NaCl + Ca(NO_3)_2 + H_2O$ Solutions

Heating $Ca(NO_3)_2{\cdot}4H_2O$ causes it to melt in its water of crystallization at ≈ 50 °C yielding a clear solution. The mixtures of $NaCl + Ca(NO_3)_2 + H_2O$ were prepared by adding known masses of solid $Ca(NO_3)_2{\cdot}4H_2O$ and NaCl to the boiling temperature apparatus followed by heating of the mixture to evaporate excess water. Heating these mixtures above ≈ 50 °C yielded a clear homogeneous solution without a solid phase. There was no distinct sudden appearance of precipitate as the solvent was evaporated by heating to higher temperatures, but rather the boiling solutions first became very faintly opaque/turbid and, with further evaporation, became cloudy will a small amount of finely divided solid phase. Upon cooling, these concentrated solutions produced an extremely viscous solution or semi-solid gel phase along with some finely divided solid. Aqueous solutions of $Ca(NO_3)_2$ are known to achieve considerable levels of oversaturation, and usually transform into a gel phase rather than precipitating a crystalline phase. According to the solubility data tabulated in Linke,[6] above about 51 °C the thermodynamically stable solid phase in contact with a saturated solution is $Ca(NO_3)_2$(cr).

An initial series of experiments was performed for $NaCl + Ca(NO_3)_2 + H_2O$ solutions in which the temperature was recorded when the boiling solutions first took on

the distinct cloudy appearance. These boiling temperatures are listed in Table III. It is apparent from these results that the measured boiling temperature is essentially constant for solutions with "as added" mole fraction compositions falling in the range $0.3000 \leq x\{\mathrm{NaCl}\} \leq 0.8000$, 164.7 ± 0.6 °C ($\sigma_{n-1}$ standard deviation). This constancy suggests that all of the solutions in this composition range have evolved to the maximum boiling temperature composition in which both solid NaCl and $Ca(NO_3)_2$ are present. However, in view of the discussion in the preceding paragraph, it can not be stated with certainty whether the $Ca(NO_3)_2$ is present as a crystalline or gel phase.

A second series of experiments was performed in which the temperature was recorded at the time the boiling solutions first took on the faintly opaque/turbid appearance. These results are reported in Table IV and are plotted in Fig. 5.c. For these measurements, because only a very small amount of solid phase was present, the "as added" mole fraction compositions should be very close approximations to the true solution mole fraction compositions. It is apparent from Fig. 5.c that the mixtures with $0.3000 \leq x\{\mathrm{NaCl}\} \leq 1$ form a smooth and continuous curve, as do the measurements with $0.8000 \leq x\{Ca(NO_3)_2\} \leq 1$. Extrapolation of these two curves indicates they would intersect at $x\{\mathrm{NaCl}\} \approx 0.25$ and $x\{Ca(NO_3)_2\} \approx 0.75$ with a boiling temperature between 165 and 170 °C.

Comparison of the results from the two series of experiments gives rise to the following interpretation of the measured boiling temperatures. The boiling temperatures of Table IV for the mole fraction composition range $0.3000 \leq x\{\mathrm{NaCl}\} \leq 1$ correspond to the presence of a solid phase of NaCl(cr). This is supported by the fact that the curve of boiling temperature *versus* $x\{\mathrm{NaCl}\}$ in this composition range extrapolates smoothly to the boiling temperature of the binary saturated solution of aqueous NaCl as $x\{\mathrm{NaCl}\} \rightarrow 1$. Similarly, the boiling temperatures of Table IV for the composition range $0.8000 \leq x\{ Ca(NO_3)_2l\} \leq 1$

correspond to the present of a solid phase of $Ca(NO_3)_2$(cr), because the boiling temperatures of these mixtures extrapolate smoothly to the boiling temperature of the binary saturated solution of aqueous $Ca(NO_3)_2$. Furthermore, the temperature at which the two curves shown in Fig. 5c intersect occurs right in the range of the maximum boiling temperatures reported in Table III. Thus the maximum boiling temperature composition for saturated solutions in the NaCl + $Ca(NO_3)_2$ + H_2O system occurs at x{NaCl} ≈ 0.25 and $x\{Ca(NO_3)_2\}$ ≈ 0.75 with a maximum boiling temperature of 164.7 ± 0.6 °C.

3.1.4. NaCl + $NaNO_3$ + KNO_3 + H_2O Solutions

An estimate was made of the mole fraction composition at which saturated solutions of NaCl + $NaNO_3$ + KNO_3 + H_2O will have their maximum boiling temperature, based on the measured boiling temperatures for the NaCl + KNO_3 + H_2O and $NaNO_3$ + KNO_3 + H_2O subsystems. The maximum boiling composition for saturated solutions in the NaCl + KNO_3 + H_2O system was found to occur at "as added" solute mole fractions of x(NaCl) ≈ 0.32 and $x(KNO_3)$ ≈ 0.68, and it was assumed that the maximum boiling composition will also occur at the same values of x(NaCl) for NaCl + $NaNO_3$ + KNO_3 mixtures. Because of the probable precipitation of KCl as described in section 3.1.2, this assumption will not be very accurate, but it allowed us to choose a starting composition for the three salt mixtures Likewise, the relative proportions of $NaNO_3$ and KNO_3 in the NaCl + $NaNO_3$ + KNO_3 + H_2O mixtures was estimated to be 0.46:0.54 from the $NaNO_3$ + KNO_3 + H_2O boiling temperature measurements.

The estimated "as added" mole fraction composition of the maximum boiling saturated three salt system is thus x(NaCl) ≈ 0.320, $x(NaNO_3)$ ≈ 0.313, and $x(KNO_3)$ ≈ 0.367. Boiling temperatures results for saturated NaCl + $NaNO_3$ + KNO_3 + H_2O solutions with this $NaNO_3/KNO_3$ ratio and with variable mole fractions of NaCl range from 154 °C

to 196 °C for x(NaCl) = 0 to 0.2299 and increase as the mole fraction of NaCl increases, see Fig. 6. A mixture was subsequently prepared with x(NaCl) = 0.50002, which is a much higher mole fraction than for the predicted maximum boiling composition of x(NaCl) = 0.32, and it should contain a significant excess of solid NaCl. The measured boiling temperature of 119.8 °C is much lower than observed in the earlier experiments, which indicates that the maximum boiling temperature composition for the saturated solutions in the NaCl + $NaNO_3$ + KNO_3 + H_2O system will occur somewhere within the range $0.230 \leq x(\text{NaCl}) < 0.500$. Another series of measurements with a $NaNO_3/KNO_3$ mole ratio of near unity (1:1.01) gave parallel but slightly lower results as shown in Fig. 6. The scatter in boiling temperatures shown in Fig. 6 is probably the result of different (and unknown) amounts of precipitation of sylvite, resulting in changes in the relative amounts of salts present in the solution phase, which cannot be accommodated on this plot. Because of the uncertainty in solution compositions, our presentation of these results is limited to Fig. 6.

A solution having the predicted maximum boiling temperature composition with "as added" $x(\text{NaCl}) \approx 0.320$, $x(NaNO_3) \approx 0.313$, and $x(KNO_3) \approx 0.367$ was also prepared, and heating the mixture gave saturated solutions whose boiling temperatures gradually increased as more solid dissolved. Between about 200 and 260 °C little solid remained, but the solution was opaque (turbid) and boiling vigorously. As the temperature was further increased, the rate of boiling decreased and the solution gradually became clear. By 300 °C the boiling has ceased and did not reoccur as the solution temperature was further increased. A repeat experiment with very nearly the same composition gave a very similar temperature of 297 °C when boiling ceased. See the first two experiments of Table V. As described in Section 2.4, the anhydrous NaCl + $NaNO_3$ + KNO_3 mixture has a melting/freezing temperature of 218 ± 3 °C.

The observations described in the preceding paragraph clearly indicate that for the composition with "as added" $x(NaCl) \approx 0.320$, $x(NaNO_3) \approx 0.313$, and $x(KNO_3) \approx 0.367$, any $NaNO_3 + KNO_3$ mixture present in the solid phase melts by about 220 °C and the excess NaCl gradually dissolves in the resulting solution as the temperature is further increased, yielding a molten salt mixture containing dissolved water. The observed cessation of boiling at 297 and 300 °C apparently corresponds to the evaporation of the last water from the molten salt mixture to yield an anhydrous molten salt. Thus, the observed temperatures of 297 to 300 °C should be considered as the dry out temperature for the $NaCl + NaNO_3 + KNO_3$ system.

In summary, an estimate was made of the $NaCl + NaNO_3 + KNO_3 + H_2O$ composition where the maximum boiling temperature might occur, based on the maximum boiling temperatures measured for constituent two salt mixtures. However, because of the probable precipitation of KCl from these solutions, there is some uncertainty in the amount of chloride needed. Mixtures were prepared with the expected $NaNO_3$ to KNO_3 mole ratio of 0.46:0.54, but because of the uncertainty the mole fraction of NaCl was varied from $x(NaCl) = 0$ to 0.5000. Mixtures with "as added" $x(NaCl) = 0$ to 0.2299 and $x(NaCl) = 0.5000$ had solid phases with saturated solution boiling temperatures ranging from 119.8 to 196 °C. However, at the estimated maximum boiling temperature composition of $x(NaCl) \approx 0.320$, $x(NaNO_3) \approx 0.313$, and $x(KNO_3) \approx 0.367$, the system forms a molten salt with a melting temperature of 218 ± 3 °C, that becomes anhydrous when heated to 297 to 300 °C.

There was no obvious evolution of gases (other than water vapor) from these high temperature solutions, no color changes in the solutions, nor was the odor of chlorine or nitrogen oxides detected. Furthermore, the residue from one of these high temperature experiments was analyzed for the presence for nitrite ions by ion chromatography and none

was detected. This information implies that no significant sample decomposition occurred during the boiling temperature / dry out temperature experiments.

3.1.5. $NaCl + NaNO_3 + KNO_3 + Ca(NO_3)_2 + H_2O$ Solutions

As described in the preceding section, the $NaCl + NaNO_3 + KNO_3 + H_2O$ mixture with "as added" $x(NaCl) \approx 0.320$, $x(NaNO_3) \approx 0.313$, and $x(KNO_3) \approx 0.367$ yields a molten salt mixture containing dissolved H_2O that becomes anhydrous when heated to about 300 °C. All of the $NaCl + NaNO_3 + KNO_3 + Ca(NO_3)_2 + H_2O$ mixtures investigated have the same mole ratio of $NaCl/NaNO_3/KNO_3$, and it is therefore not surprising that all of studied $NaCl + NaNO_3 + KNO_3 + Ca(NO_3)_2 + H_2O$ mixtures form molten salts with dissolved water that become anhydrous at high temperatures.

Table V lists the dry out temperatures for the $NaCl + NaNO_3 + KNO_3 + Ca(NO_3)_2 + H_2O$ mixtures, where the molten salt mixtures are anhydrous above these temperatures, and Fig. 5.d is a plot of these results. The dry out temperatures increase rapidly with increasing values of $x\{Ca(NO_3)_2\}$, from $x\{Ca(NO_3)_2\} = 0$ to 0.1500. The dry out temperature for the mixtures with $x\{Ca(NO_3)_2\} = 0.2000$ and 0.2500 are even higher, > 400 °C, but the exact dry out temperatures could not be determined because they exceed the 400 °C upper limit of our temperature measuring system. However, boiling was extremely slow for these solutions at 400 °C, which implies that the dry out temperatures for these two experiments are only slightly higher than this. It should be noted that because the solutions at the dry out temperatures are molten salts, the mole fractions of the solute components are identical to those calculated from the masses of added salt.

3.2. Deliquescence Relative Humidity

Figures 7 and 8 show the resistivity changes that were recorded for the mutual deliquescence/efflorescence relative humidity determinations for $NaNO_3$ + KNO_3 and NaCl + $NaNO_3$ + KNO_3 salt mixtures, respectively, from 120 to 180 °C, and Table VII reports the numerical results. The observed drops in impedance clearly indicate that absorption of water vapor by the salt assemblage is occurring. Figure 8 shows a three to four decade drop in impedance for NaCl + $NaNO_3$ + KNO_3 salt mixtures at a MDRH of 25.9% at 120 °C and 10.5% at 180 °C indicating the formation of a brine solution at temperatures much higher than the predicted dry out temperatures from thermodynamic modeling calculations using EQ3/6,[10] of about 140 °C at 1 bar (136 °C at 0.9 bar).[1] The mismatches between the EQ3/6 model calculations (blue and red curves) and our experimental results for $NaNO_3$ + KNO_3 and NaCl + $NaNO_3$ + KNO_3 salt mixtures are largely due to uncertainties in the model predictions resulting from the unavailability of some of the Pitzer model parameters at these higher temperatures, as described in the Introduction. As expected, there is a decrease in the MDRH occurring with increasing temperature. Deliquescence of the salt mixture is reversible as indicated by the general agreement between the MDRH and MERH values reported in Table VII. Generally, the measured mutual efflorescence relative humidity is about 1% RH unit below the measured mutual deliquescence relative humidity at a specific temperature.

Figure 7 shows a three to four decade drop in impedance for $NaNO_3$ + KNO_3 salt mixture at MDRH of 26.4% at 120 °C and 20.0% at 150 °C. The generally good agreement between MDRH and MERH values shows that deliquescence of the $NaNO_3$ + KNO_3 mixtures is a reversible process. As was the case with the three salt mixtures, the MERH is about 1 %RH unit below the MDRH. At each temperature the $NaNO_3$ + KNO_3 two salt mixtures deliquesce at slightly higher relative humidities (0.4 to 2 % RH units)

than the three salt NaCl + $NaNO_3$ + KNO_3 mixtures. One possible explanation for the similar MDRH/MERH values for these two systems is that the NaCl + $NaNO_3$ + KNO_3 system is dominated by potassium nitrate and sodium nitrate chemistry. This explanation is supported by high nitrate to chloride ratios measured near the eutonic composition for the NaCl + $NaNO_3$ and NaCl + KNO_3 mixtures.[5,9] Addition of NaCl to the nitrate salts stabilizes the brines to higher temperatures.

The $NaNO_3$ + KNO_3 salt mixture should not deliquescence above its maximum boiling temperature of 165 °C for saturated $NaNO_3$ + KNO_3 + H_2O solutions. However, our experiments show that the $NaNO_3$ + KNO_3 salt mixtures still absorb some water at 180 °C (Fig. 7, Table VII). We do not believe that one to two decade drop in impedance is an artifact due to changes in temperature of the experiment. It is possible that the observed one to two decade drop in impedance at 180 °C reflects the absorption of surface layers of water rather than actual deliquescence observed in boiling point and solubility experiments. This explanation is consistent with the observed absorption of water at relative humidity lower than the equilibrium deliquescence RH in similar salt mixtures reported by Ge *et al.*[22] and Yang *et al.*[19]

However, another possibility exists. In the maximum boiling temperature experiments the solid phase was that obtained from precipitation upon cooling of a solution used in a previous high boiling temperature experiment. This solid phase present for the maximum boiling temperature experiment was probably the thermodynamically-favored solid solution $Na_xK_{1-x}NO_3$(ss). In contrast, for the MDRH/MERH measurement with the resistivity cell, the solid phase may have been the metastable eutonic mixture of $NaNO_3$(cr) + KNO_3(cr). The solubility of the metastable eutonic mixture of $NaNO_3$(cr) + KNO_3(cr), and thus its maximum MDRH/MERH temperature, should be higher than

those for $Na_xK_{1-x}NO_3$(ss). The RH value obtained at 180 °C is ≈ 3.5 % below the value estimated by linear extrapolation of MDRH/MERH values at 120 to 150 °C, see Fig. 9, which slightly exceeds the combined experimental uncertainty. This fair agreement suggests that the resistivity change at 180 °C could possibly be due to deliquescence of the metastable eutonic mixture of $NaNO_3$(cr) + KNO_3(cr) that is unable to transform to the stable $Na_xK_{1-x}NO_3$(ss) during the timeframe of the MDRH/MERH experiments. At this time it is not possible to distinguish between this possibility and the surface absorption of water.

3.3. Conclusions from the Combined Measurements

The vapor pressure of a saturated single salt solution in equilibrium with a particular solid phase (hydrated or unhydrated) corresponds to the MDRH/MERH for that phase, and the boiling temperature of the saturated solution is the maximum temperature at which mutual deliquescence / efflorescence can occur at the confining pressure. For a mixed salt system, the maximum boiling temperature that can occur for the saturated mixtures corresponds to the MDRH/MERH of the eutonic composition at the highest temperature at which deliquescence can occur at the particular confining pressure (in our case, ambient pressure). That is, the MDRH/MERH is equal to the ambient pressure divided by the vapor pressure of pure water at the maximum boiling temperature. Thus, the relative humidity of the solution at the boiling temperature corresponds to the upper limit on a plot of the MDRH/MERH as a function of temperature.

Figure 9 is a plot of the MDRH/MERH results for the NaCl + KNO_3, $NaNO_3$ + KNO_3, and NaCl + $NaNO_3$ + KNO_3 systems as a function of temperature. The saturation relative humidities of pure H_2O at a confining pressure of 1 atmosphere (0.101325 MPa)

on this plot were taken from Table VI, and are based on water vapor pressures of water from the Handbook of Chemistry of Chemistry and Physics.[14] The directly measured values of the MDRH/MERH for the $NaNO_3 + KNO_3$ system from Table VII and those from Carroll *et al.*[9] for the $NaCl + KNO_3$ system both connect fairly well with the values obtained from the maximum boiling temperatures of saturated solutions from Tables I and II, with the boiling temperature results falling 1 to 2% RH units lower than those extrapolated from the MDRH/MERH measurements (and have better agreement with the MERH data). The agreement between these two types of measurements is within their combined experimental uncertainties. This plot shows that these two different types of measurements yield results that are consistent within their experimental errors, and thus the combined curves can be used to reliably estimate MDRH/MERH values at other temperatures. The maximum boiling temperature for the $NaCl + NaNO_3 + KNO_3$ system cannot be directly related to the MDRH/MERH from Table VII because of the occurrence of the low melting solid phase, but the melting temperature determined for this mixture provides the upper temperature limit at which deliquescence of the solid mixture could occur.

The combined results for the $NaCl + KNO_3$ and the $NaNO_3 + KNO_3$ systems, and the boiling temperatures $NaCl + Ca(NO_3)_2$ system, indicate that liquid solutions can form by deliquescence at temperatures of 135 to 165°C. However, for the $NaCl + NaNO_3 + KNO_3$ system, liquid solutions exist in equilibrium with the solid phase up to the melting temperature of 218 ± 3 °C, and molten salts containing water can exist at higher temperatures for this and the $NaCl + NaNO_3 + KNO_3 + Ca(NO_3)_2 + H_2O$ system. Thus these three- and four-salt mixtures can form concentrated brine solutions even above the

highest temperatures envisioned for the proposed Yucca Mountain Nuclear Waste Repository.

4. SUMMARY

Boiling temperature were measured for saturated solutions in the NaCl + KNO_3 + H_2O, $NaNO_3$ + KNO_3 + H_2O, and NaCl + $Ca(NO_3)_2$ + H_2O systems at ambient pressure. The observed maximum boiling temperatures for these systems are 134.9 °C, 165.1 °C, and 164.7 ± 0.6 °C, respectively. The uncertainties of the first two boiling temperatures are estimated as being between 0.5 and 1.0 K. Dry out temperatures of $t \geq 300$ °C were also determined for the NaCl + $NaNO_3$ + KNO_3 + $Ca(NO_3)_2$ + H_2O system, which correspond to the temperatures at which the molten salt plus water mixture ceases to boil and becomes anhydrous. Mutual deliquescence/efflorescence relative humidity were determined for NaCl + KNO_3 + $NaNO_3$ and KNO_3 + $NaNO_3$ salt mixtures from 120 to 180 °C.

ACKNOWLEDGMENTS

This work was performed under the auspices of the U. S. Department of Energy by University of California, Lawrence Livermore National Laboratory under contract No. W-7405-ENG-48. This work is supported by the U.S. Department of Energy, Office of Repository Development. We thank Dr. Peter Huang (National Institute of Standards and Technology, Gaithersburg) for numerous helpful discussions related to the design of the bi-thermal apparatus used for calibrating the relative humidity probes.

REFERENCES

1. *Environment on the Surfaces of the Drip Shield and Waste Package Outer Barrier*. Report ANL-EB-MD-000001 REV 01 (Bechtel SAIC Company, Las Vegas, Nevada, 2004).

2. *General Corrosion and Localized Corrosion of Waste Package Outer Barrier*. Report ANL-EB-MD-000002 REV 02 (Bechtel SAIC Company, Las Vegas, Nevada, 2004).

3. J. J. Gray, J. R. Hayes, G. E. Gdowski, and C. A. Orme, Inhibiting Effects of Nitrates on the Passive Film Breakdown of Alloy 22 in Chloride Solutions, *J. Electrochem. Soc*., accepted for publication.

4. N. D. Rosenberg, G. E. Gdowski, and K. G. Knauss, Evaporative Chemical Evolution of Natural Waters at Yucca Mountain, Nevada, *Appl. Geochem.* **16**, 1231–1240 (2001).

5. M. Alai, M. Sutton, and S. Carroll, Evaporative Evolution of a Na–Cl–NO_3–K–Ca–SO_4–Mg–Si Brine at 95 °C: Experiments and Modeling Relevant to Yucca Mountain, Nevada, *Geochem. Trans*. **6**, 31–45 (2005); S. Carroll, M. Alai, L. Craig, G. Gdowski, P. Hailey, Q. A. Nguyen, J. Rard, K. Staggs, M. Sutton, and T. Wolery, *Chemical Environment at Waste Package Surfaces in a High-Level Radioactive Waste Repository*, Report UCRL-TR-212566 (Lawrence Livermore National Laboratory, Livermore, California, 2005).

6. W. F. Linke, *Solubilities, Inorganic and Metal-Organic Compounds*, fourth ed. (American Chemical Society, Washington, D.C., 1958); Vol. I, pp. 615, 616.

7. W. F. Linke, *Solubilities, Inorganic and Metal-Organic Compounds*, fourth ed. (American Chemical Society, Washington, D.C., 1965); Vol. II, pp. 250, 261–263, 265, 266, 958, 959, 1069, 1070.

8. L. Craig, S. Carroll, and T. Wolery, Deliquescence of NaCl-$NaNO_3$ and KNO_3-$NaNO_3$ Salt Mixtures at 90°C, in *Water–Rock Interaction*, Proceedings of the Eleventh International Symposium on Water–Rock Interaction (A. A. Balkema Publishers, Leiden, The Netherlands, 2004); Vol. 2, pp. 1275–1278.

9. S. Carroll, L. Craig, and T. J. Wolery, Deliquescence of NaCl-$NaNO_3$, KNO_3-$NaNO_3$, and NaCl-KNO_3 Salt Mixtures from 90 to 120 °C, *Geochem. Trans*. **6**, 19–30 (2005).

10. T. J. Wolery and R. L. Jarek, *EQ3/6, Version 8.0, Software User's Manual*, Software Document Number 10813-UM-8.0-00 (U. S. Department of Energy, Office of Civilian Radioactive Waste Management, Office of Repository Development, 1261 Town Center Drive, Las Vegas, Nevada 89144, January 2003).
11. K. S. Pitzer, in *Activity Coefficients in Electrolyte Solutions*, second ed., Pitzer, K. S., Ed. (CRC Press, Boca Raton, Florida, 1991), Chapter 3.

12. J. A. Rard, *Results from Boiling Temperature Measurements for Saturated Solutions in the Systems NaCl + KNO_3 + H_2O, $NaNO_3$ + KNO_3 + H_2O, and NaCl + $NaNO_3$ + KNO_3 + H_2O*, Report UCRL-TR-207054 (Lawrence Livermore National Laboratory, Livermore, California, 2004).
13. J. A. Rard, *Results from Boiling Temperature Measurements for Saturated Solutions in the Systems NaCl + $Ca(NO_3)_2$ + H_2O, $NaNO_3$ + KNO_3 + H_2O, and NaCl + KNO_3 + H_2O, and Dry Out Temperatures for NaCl + $NaNO_3$ + KNO_3 + $Ca(NO_3)_2$ + H_2O*, Report UCRL-TR-?????? (Lawrence Livermore National Laboratory, Livermore, California, 2005).
14. R. C. Weast (Editor-in-Chief) *CRC Handbook of Chemistry and Physics* (CRC Press, Boca Raton, Florida, 1987–1988), pages B-119, B-130, B-131, D-189, D-190.
15. J. Timmermans, *The Physico-chemical Constants of Binary Systems in Concentrated Solutions* (Interscience, New York City, New York, 1960); Vol. 3, pp. 155, 156, 306, 307, 387, 388, 554, 555, 778.
16. J. A. Rard, Isopiestic Determination of the Osmotic Coefficients of $Lu_2(SO_4)_3$(aq) and H_2SO_4(aq) at the Temperature T = 298.15 K, and Review and Revision of the Thermodynamic Properties of $Lu_2(SO_4)_3$(aq) and $Lu_2(SO_4)_3 \cdot 8H_2O$(cr), *J. Chem. Thermodyn.* **28**, 83–110 (1996).
17. R. A. Robinson and R. H. Stokes, *Electrolyte Solutions*, second ed. (revised) (Butterworth & Co., London, 1965); Appendix 8.11, Table 2.
18. R. T. Pabalan, L. Yang, and L. B. Browning, *Effects of Salt Formation on the Chemical Environment of Drip Shields and Waste Packages at the Proposed Nuclear Waste Repository at Yucca Mountain, Nevada*, Report CNWRA 2002-03 (Center for Nuclear Waste Regulatory Analyses, San Antonio, Texas, May 2002).

19. L. Yang, R. T. Pabalan, and L. Browning, Experimental Determination Of the Deliquescence Relative Humidity and Conductivity of Multicomponent Salt Mixtures, in *Scientific Basis for Nuclear Waste Management XXV*, Materials Research Society

Proceedings Volume 713, P. McGrail and G. A. Cragnolino, eds. (Materials Research Society, Warrendale, Pennsylvania, 2002), pages 135–142.
20. R. H. Stokes, The Measurement of Vapor Pressures of Aqueous Solutions by Bi-thermal Equilibration Through the Vapor Phase, *J. Am. Chem. Soc*. **69**, 1291–1296 (1947).
21. W. W. Ewing, Calcium Nitrate. II. The Vapor Pressure-Temperature Relations of the Binary System Calcium Nitrate-Water, *J. Am. Chem. Soc*. **49**, 1963–1973 (1927).
22. Z. Ge, A. S. Wexler, and M. V. Johnston, Deliquescence Behavior of Multicomponent Aerosols, *J. Phys. Chem. A* **102**, 173–180 (1998).

Table I. Boiling Temperatures for Saturated Aqueous Solutions of NaCl, $NaNO_3$, KNO_3, and $Ca(NO_3)_2$, and the Maximum Boiling Mixture of NaCl + KNO_3 + H_2O

x{NaCl}	x{$NaNO_3$}	x{KNO_3}	x{$Ca(NO_3)_2$}	pressure/ bar	temperature/°C corrected
1.0000	0	0	0	0.991±0.005[a]	107.7±0.2 [a]
0	1.0000	0	0	0.994±0.001[b]	119.7±0.4[b]
0	0	1.0000	0	0.992±0.0.002[c]	114.6_5±0.5[c]
0	0	1.0000	0	0.998±0.002[d]	115.3±0.8[d]
0	0	1.0000	0	0.995±0.005[e]	115.0±0.7[e]
0	0	0	1.0000	0.998±0.001[f]	150.2±0.0[f]
unknown	0	unknown		0.9958	134.9 [g]

[a] This is the average of ten determinations for NaCl + H_2O.

[b] This is the average of six determinations for $NaNO_3$ + H_2O.

[c] This is the average of the four determinations for KNO_3 + H_2O at lower pressures.

[d] This is the average of the five determinations for KNO_3 + H_2O at higher pressures.

[e] This is the average of all nine determinations for KNO_3 + H_2O.

[f] This is the average of two determinations for $Ca(NO_3)_2$ + H_2O.

[g] A solution having the starting composition x(NaCl) = 0.5001 and x(KNO_3) = 0.4999 was boiled down until the maximum boiling temperature composition was reached. This boiling temperature corresponds to MDRH/MERH = 31.9 ± 0.7 % assuming that the temperature uncertainty is 0.7_5 °C.

Table II. Boiling Temperatures for Saturated Aqueous Solutions of $NaNO_3$ + KNO_3 + H_2O

$x(NaNO_3)$	$x(KNO_3)$	pressure (bar)	temperature/°C corrected
0	1.0000	0.995±0.005	115.0±0.7 [a]
0.0523	0.9477	0.9918	116.5
0.1085	0.8915	0.9918	119.3
0.1665	0.8335	0.9919	122.6
0.1665	0.8335	0.9951	123.5 [b]
0.2205	0.7795	0.9950	127.2
0.2500	0.7500	1.0061	129.6
0.2729	0.7271	0.9947	131.0
0.3334	0.6666	0.9947	136.1
0.3619	0.6381	0.9947	143.7
0.4329	0.5671	0.9906	154.8
0.4568	0.5432	0.9957	152.7
0.4568	0.5432	0.9964	158.8 [b]
0.4568	0.5432	0.9964	159.0 [b]
0.4568	0.5432	0.9964	159.8 [b]
0.4568	0.5432	0.9968	159.7 [b]
0.4569	0.5431	0.9946	154.3
0.4569	0.5431	0.9935	160.5 [b]
0.4804	0.5196	0.9908	153.4
0.4982	0.5018	0.9966	152.3
0.5001	0.4999	1.0047	163.6

unknown	unknown	1.0047	165.1 [c]
0.5545	0.4455	0.9912	147.2
0.6207	0.3793	0.9912	140.4
0.6895	0.3105	0.9948	132.4
0.6895	0.3105	0.9914	134.8 [b]
0.7500	0.2500	0.9915	129.4
0.7500	0.2500	0.9939	129.3 [b]
0.7732	0.2268	0.9949	128.1
0.8419	0.1581	0.9949	125.2
0.9007	0.0993	0.9949	122.5
0.9516	0.0484	0.9949	120.9
1.0000	0	0.994±0.001[d]	119.7±0.4 [d]

[a] This is the average of nine determinations for $KNO_3 + H_2O$ reported in Table I. [b] This initial composition of this solution is identical to the one immediately above. These measurements involved partial dissolution of the glassy-looking solid that was produced after the solution from the previous experiment cooled to room temperature. These variations in boiling temperatures for the re-equilibrated solutions reflect small changes in the composition of the solid phase, and, above about 150 °C, the gradual transformation of the discreet solid phases $NaNO_3$(s) and KNO_3(s) into a solid solution. [c] The previous solution having the starting composition $x(NaNO_3) = 0.5001$ and $x(KNO_3) = 0.4999$ was boiled down until the maximum boiling temperature composition was reached. This boiling temperature corresponds to MDRH/MERH = 14.3 ± 0.3 % assuming that the temperature uncertainty is 0.7_5 °C. [d] This is the average of six determinations for $NaNO_3 + H_2O$ reported in Table I.

Table III. Boiling Temperatures for Saturated Aqueous Solutions of NaCl + $Ca(NO_3)_2$ + H_2O[a]

x{NaCl}	$x\{Ca(NO_3)_2\}$	pressure/ bar	temperature/°C corrected
0	1.0000	0.998±0.001[b]	150.2±0.0 [b]
0.1000	0.9000	0.9976	154.2
0.1996	0.8004	0.9995	159.2
0.3000	0.7000	0.9976	164.4
0.4030	0.5970	0.9973	164.6
0.5000	0.5000	0.9948	164.6
0.6000	0.4000	0.9962	164.8
0.7000	0.3000	0.9991	164.2
0.8000	0.2000	1.0019	165.8
1.0000	0	0.991±0.005[c]	107.7±0.2 [c]

[a] The reported compositions are the solute mole fractions (not including water) that were calculated from the mass of each solute component added to the solution. The initially liquid solutions were heated to evaporate solvent until the appearance of a distinct cloudy appearance due to the formation of a solid phase. Because the amount of solid present is not known, the reported mole fractions are not an accurate reflections of the solution composition, except when $x\{Ca(NO_3)_2\} = 1$ where only a single solute is present. However, the near constancy of the boiling temperatures for solutions with "as added" compositions in the range $0.3000 \leq x\{NaCl\} \leq 0.8000$, 164.7 ± 0.6 °C ($\sigma_{n-1}$ standard deviation) suggests that all of these solutions have evolved to the maximum boiling temperature composition.

[b] This is the average of two determinations for $Ca(NO_3)_2 + H_2O$ reported in Table I.

[c] This is the average of ten determinations for NaCl + H_2O reported in Table I.

Table IV. Boiling Temperatures for Saturated Aqueous Solutions of NaCl + $Ca(NO_3)_2$ + H_2O[a]

x{NaCl}	$x\{Ca(NO_3)_2\}$	pressure/ bar	temperature/°C corrected
0	1.0000	0.998±0.001[b]	150.2±0.0 [b]
0.1000	0.9000	0.9980	155.4
0.2000	0.8000	0.9934	161.2
0.3000	0.7000	0.9995	145.8
0.4000	0.6000	1.0022	126.6
0.5000	0.5000	1.0035	119.8
0.6000	0.4000	1.0029	116.1
0.7000	0.3000	0.9978	113.1
0.8181	0.1819	1.0001	111.2
0.9000	0.1000	0.9965	109.7
0.9500	0.0500	0.9943	109.2
1.0000	0	0.991±0.005[c]	107.7±0.2

[a] The reported compositions are the solute mole fractions (not including water) that were calculated from the mass of each solute component added to the solution. The initially liquid solutions were heated to evaporate solvent until they became faintly opaque (turbid). This corresponds to the beginning of precipitation of a solid phase, and the reported mole fractions should correspond very closely to the actual solution compositions.

[b] This is the average of two determinations for $Ca(NO_3)_2 + H_2O$ reported in Table I.

[c] This is the average of ten determinations for NaCl + H_2O reported in Table I

Table V. Maximum Boiling (Dryout) Temperatures for Saturated Aqueous Solutions of $NaCl + NaNO_3 + KNO_3 + Ca(NO_3)_2 + H_2O$ (No Solid Phase)[a]

$x\{NaCl\}$	$x\{NaNO_3\}$	$x\{KNO_3\}$	$x\{Ca(NO_3)_2\}$	pressure/ bar	temperature/°C corrected
0.32002	0.31299	0.36699	0	0.9927	~300
0.32002	0.31298	0.36700	0	0.9907	~297
0.30401	0.29733	0.34865	0.05001	0.9920	~354[b]
0.30402	0.29733	0.34865	0.05000	0.9896	~315[c]
0.29602	0.28950	0.33948	0.07500	0.9900	~325[c]
0.28802	0.28168	0.33030	0.10000	0.9922	~377[c]
0.27202	0.26603	0.31195	0.15000	0.9935	~393[c]
0.25602	0.25038	0.29360	0.20000	0.9922	≥400[c,d]
0.24002	0.23473	0.27525	0.25000	0.9901	≥400[c,d]
(0.50002)[e]	(0.22999)[e]	(0.26999)[e]	0	(1.0005)[e]	(119.8)[e]

[a] The reported compositions are the solute mole fractions (not including water) that were calculated from the mass of each solute component added to the solution. The molar ratio of $NaCl:NaNO_3:KNO_3$ is essentially constant for all these solutions at 1:0.9780:1.1468 and corresponds to the maximum boiling mole fraction composition estimated from the two salt mixture data. The initial solutions plus solid phase were heated to evaporate solvent, which resulted in a molten salt containing some water. The reported temperatures are the lowest temperatures at which visible boiling ceased. At temperatures slightly above the reported values, the system consists of a clear liquid phase that does not boil, and presumably consists of the corresponding anhydrous molten salt mixture. Because all of the solutes are present in this homogeneous liquid phase, the reported mole fractions should correspond to the actual solution composition. [b] This temperature appears to be anomalously high and may be erroneous. The temperature of this experiment was high enough that the Teflon coatings of the Type T thermocouples melted off, although the thermocouples were otherwise undamaged. The following experiment, involving a

separately prepared mixture, has a lower boiling temperature more consistent with those for the other compositions. [c] The thermocouples for these experiments were type T, but were uncoated and the thermocouple wells were made of inconel. For the first three experiments in this table, the thermocouple was a coated type T thermocouple. [d] These two temperatures are very close to the dry out temperatures at these compositions, but the measuring system being used has a maximum recording temperature of 400 °C. [e]This single experiment is for a different molar ratio of $NaCl:NaNO_3:KNO_3$, with a solid phase in equilibrium with the saturated solution; the other experiments of this table were made above the melting temperature of the salt mixtures.

Table VI. Calculated Relative Humidity Standard Values for a Bi-thermal System Based on the Saturated Vapor Pressure of Water from 100 to 200 °C, Assuming the Lower Reservoir Temperature to be 100 °C

Temperature (°C)	Vapor Pressure[a]/Pa	Relative Humidity (percent)
100	101325	100.00
105	120799	83.88
110	143263	70.73
115	169050	59.94
120	198536	51.04
125	232105	43.65
130	270124	37.51
135	312942	32.38
140	361426	28.03
145	415534	24.38
150	476025	21.29
155	543406	18.65
160	618082	16.39
165	701764	14.46
170	792058	12.79
175	892471	11.35
180	1002584	10.11
185	1123086	9.02
190	1255011	8.07
195	1398386	7.25
200	1554427	6.52

[a] Values taken from the Handbook of Chemistry and Physics,[(14)] after conversion from torr (mm of mercury) to Pa.

Table VII. Experimental Mutual Deliquescence/Efflorescence Relative Humidities (MDRH/MERH) for NaCl + $NaNO_3$ + KNO_3 and $NaNO_3$ + KNO_3 Salt Mixtures from 120 to 180 °C Determined with the Resistivity Cell

Temperature/°C	%MDRH[a]	%MERH[a]
	$NaNO_3 + KNO_3$ [b]	
120	26.4±0.4	25.2±0.4
135	23.8±1.0	22.9±1.0
150	20.0±0.9	19.0±0.9
180	10.6±0.2[c]	10.6±0.2[c]
	NaCl + $NaNO_3$ + KNO_3	
120	25.9±1.0	25.0±1.0
135	21.8±0.9	20.8±0.9
150	18.1±0.9	17.1±0.9
180	10.5±0.8	10.2±0.8

[a] All %RH values have been corrected by using the calibration of the humidity probes with the bi-thermal apparatus, based on vapor pressures reported in the Handbook of Chemistry and Physics.(14)

[b] At 165.1 °C the maximum boiling temperature composition results, reported in footnote c of Table II, yield MDRH/MERH = 14.3 ± 0.3 %.

[c] Water absorption/loss occurs at these MDRH/MERH values, and possibly corresponds to deliquescence/efflorescence. However, it is also possible that the resistivity decrease observed in these experiments is simply the result of surface absorption of water.

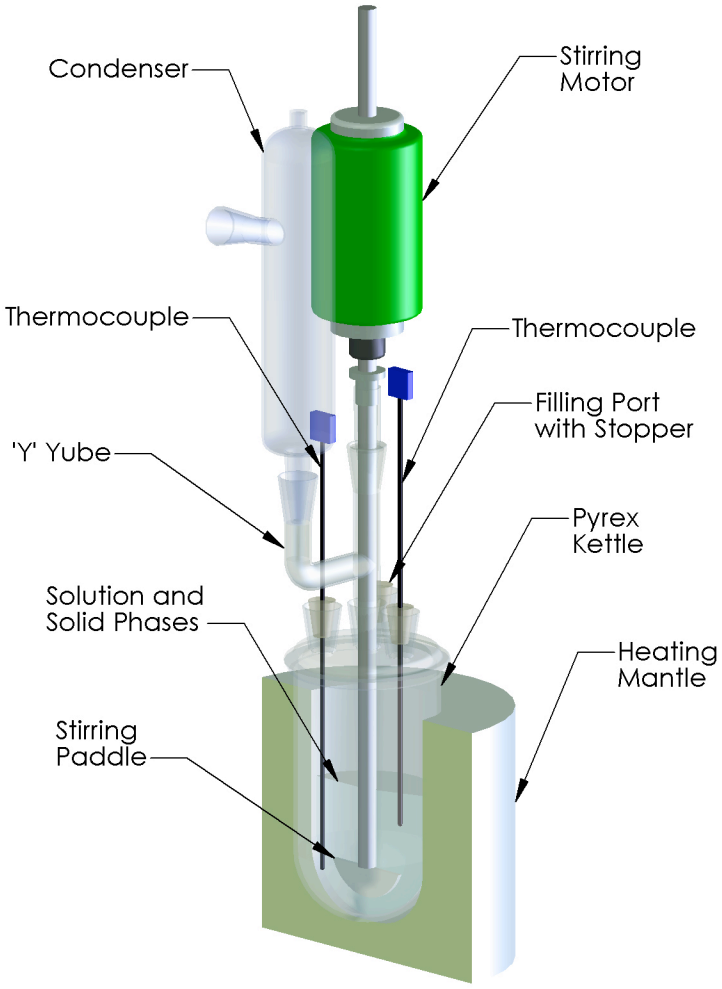

Fig. 1. Illustration of the apparatus used for determining boiling temperatures.

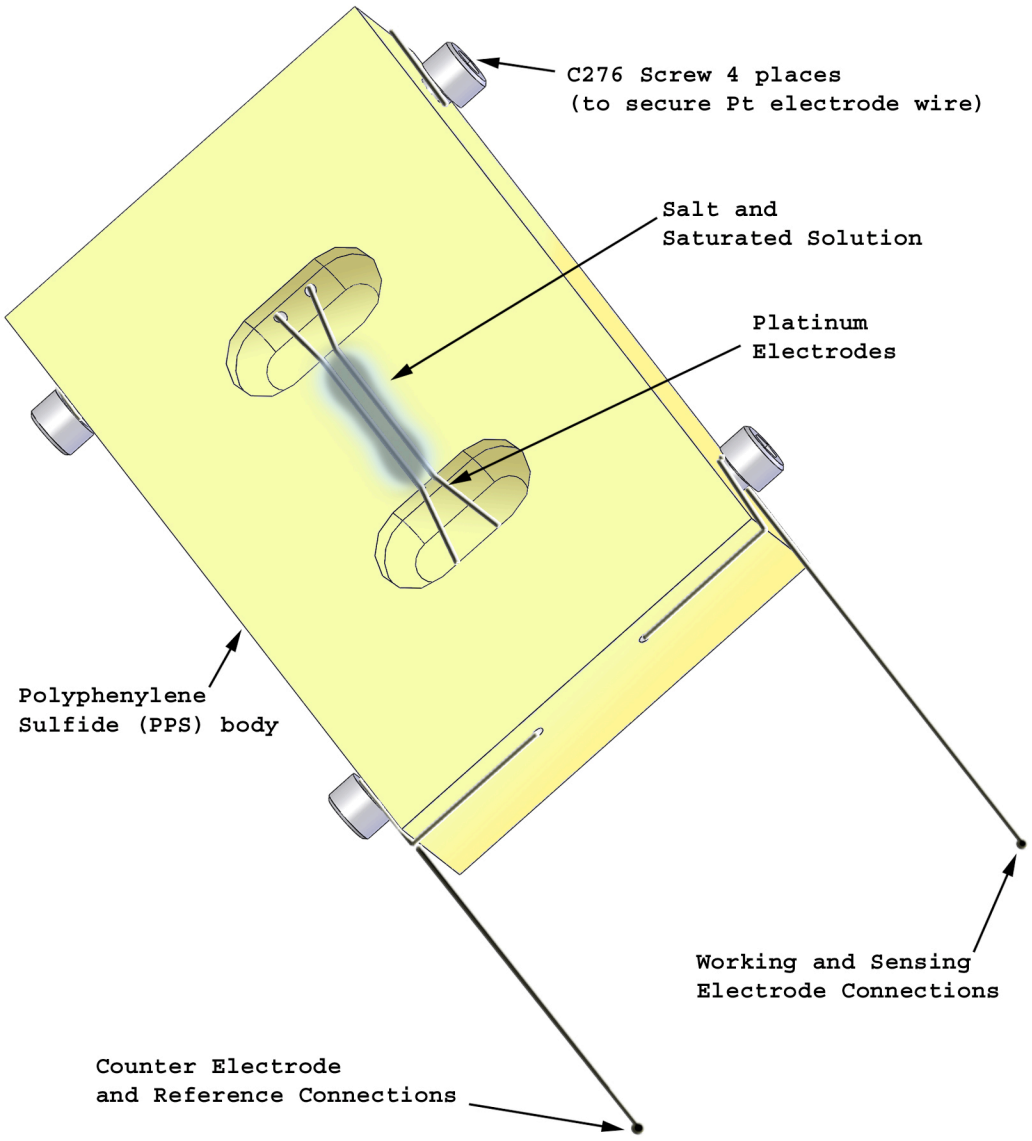

Fig. 2. Illustration of the resistivity cell for determining the MDRH/MERH values for salt mixtures.

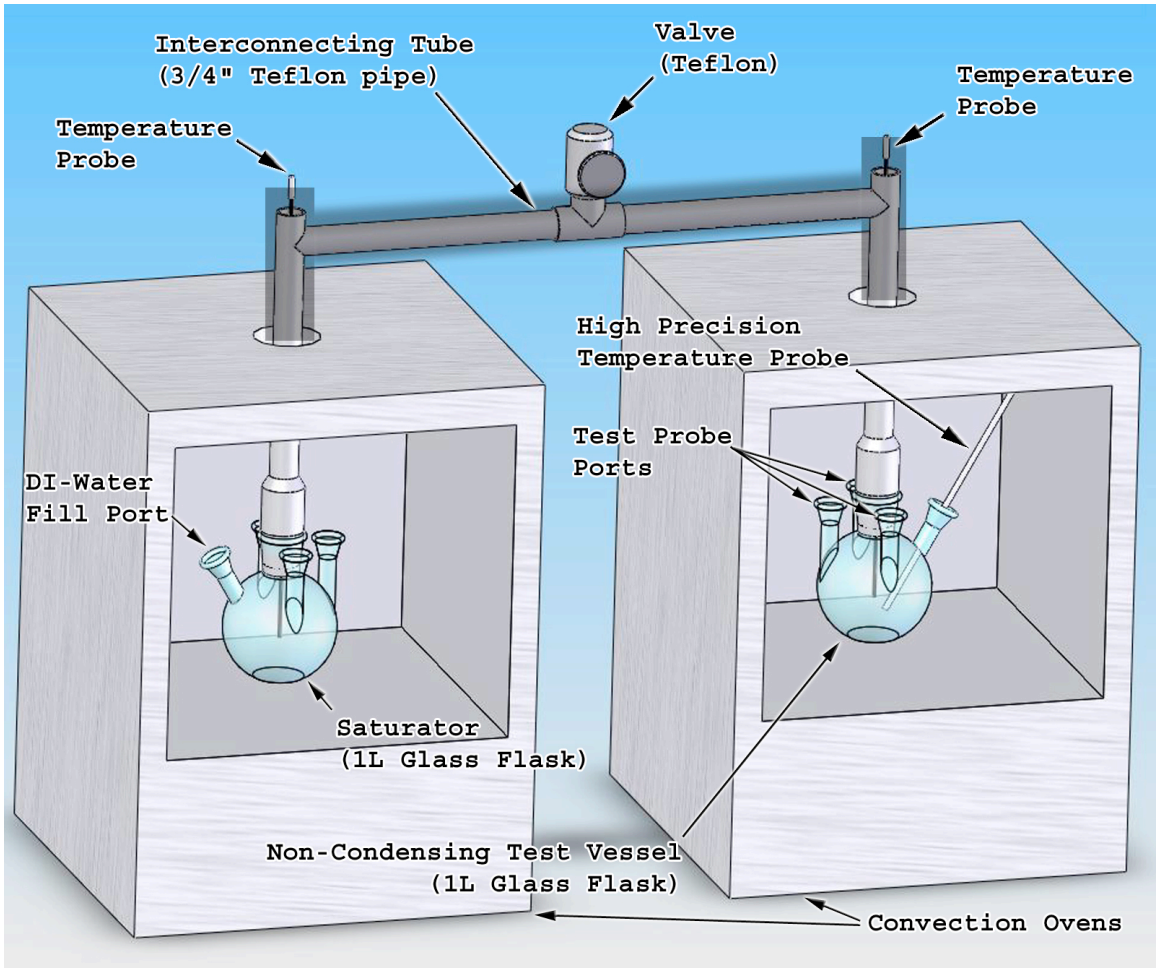

Fig. 3. Illustration of the bi-thermal apparatus used for calibration of RH probes at elevated temperature.

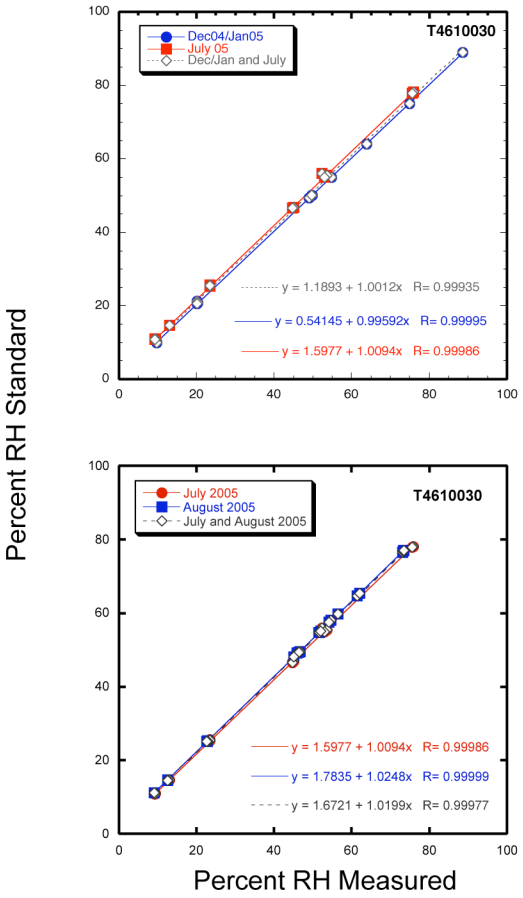

Fig. 4. Results from calibration of the relative humidity probe using the bi-thermal apparatus.

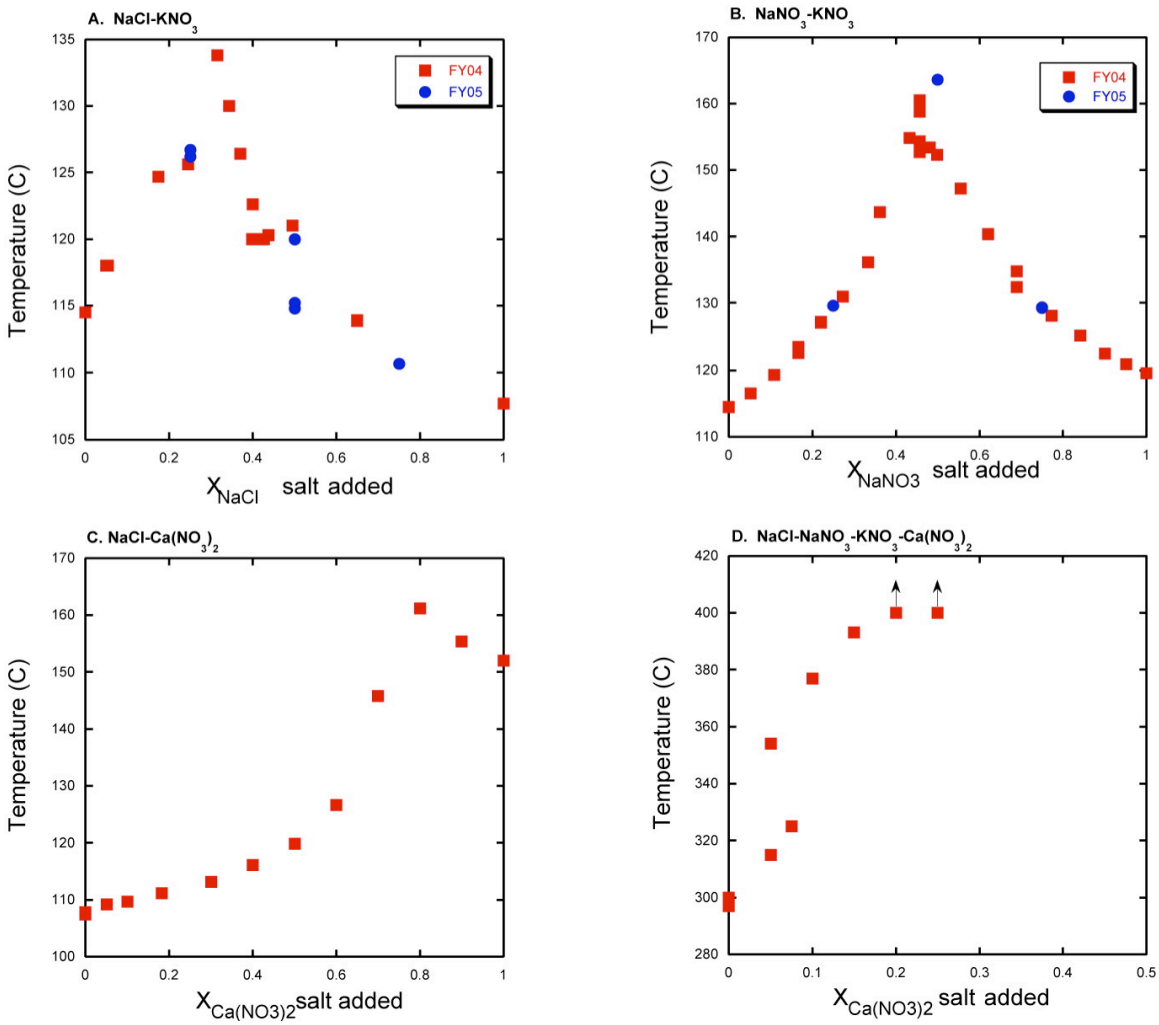

Fig. 5. a. Boiling temperatures for saturated NaCl + KNO_3 + H_2O solutions plotted against the mole fraction of NaCl added to the system. Points labeled with red squares were measured in fiscal year 2004 (FY04) and those with blue circles were measured in fiscal year 2005 (FY05). Because of the probable precipitation of KCl(cr) from these solutions, the mole fraction of added NaCl is not a meaningful representation of the solution composition and is used for convenience only. **b.** Boiling temperatures for saturated $NaNO_3$ + KNO_3 + H_2O solutions plotted against the mole fraction of $NaNO_3$ added to the system. **c.** Boiling temperatures from Table III for saturated NaCl + $Ca(NO_3)_2$ + H_2O solutions plotted against the mole fraction of $Ca(NO_3)_2$ added to the system (which should correspond closely to the actual solution mole fraction). **d.** Dry out temperatures NaCl + $NaNO_3$ + KNO_3 + $Ca(NO_3)_2$ + H_2O solutions plotted against the mole fraction of $Ca(NO_3)_2$ added to the system. At these temperatures this system forms anhydrous molten salts.

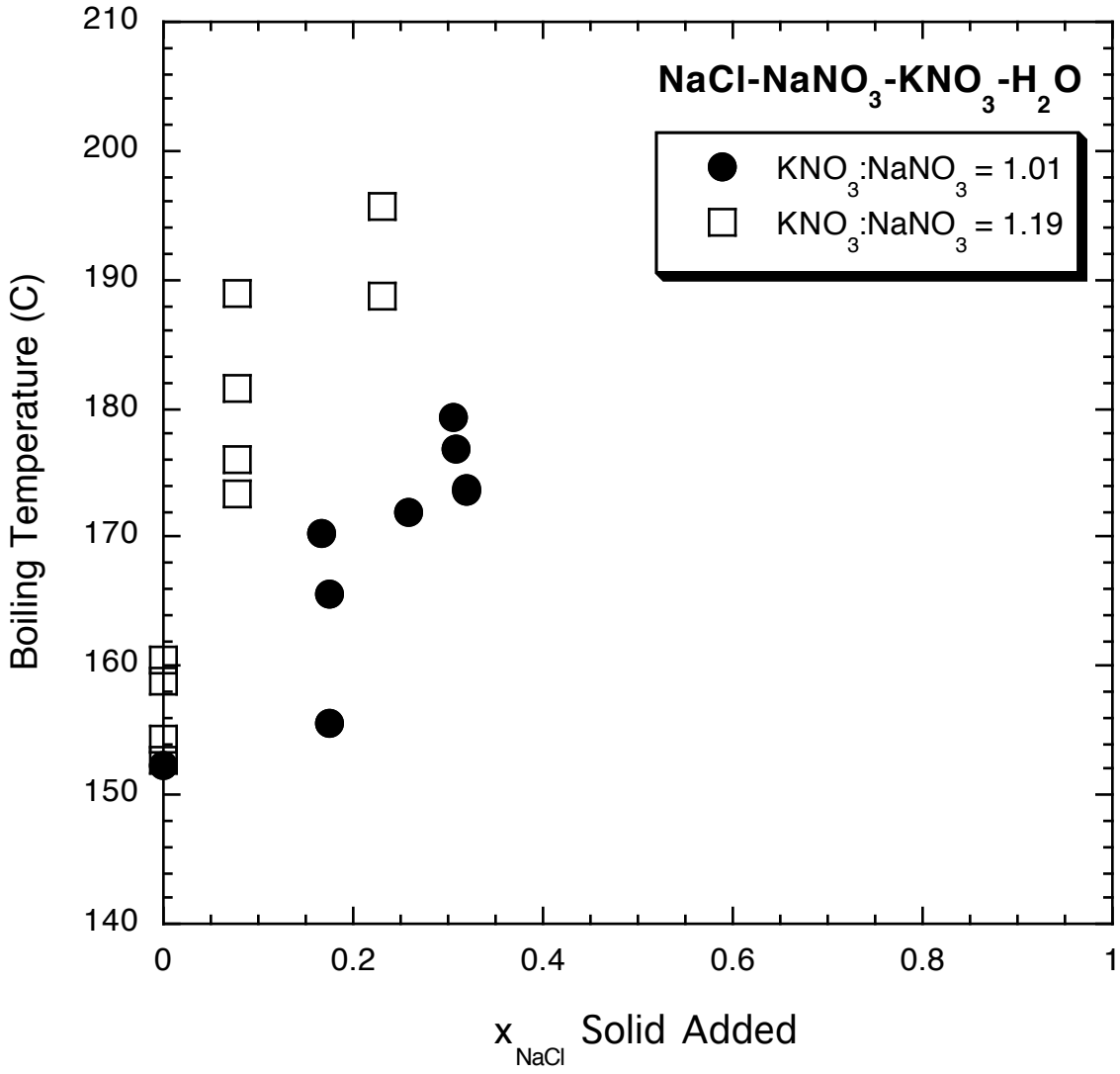

Fig. 6. Boiling temperatures for saturated NaCl + $NaNO_3$ + KNO_3 + H_2O solutions plotted against the mole fraction of NaCl added to the system, at two specific mole ratios of KNO_3:$NaNO_3$ of 1.01 and 1.19.

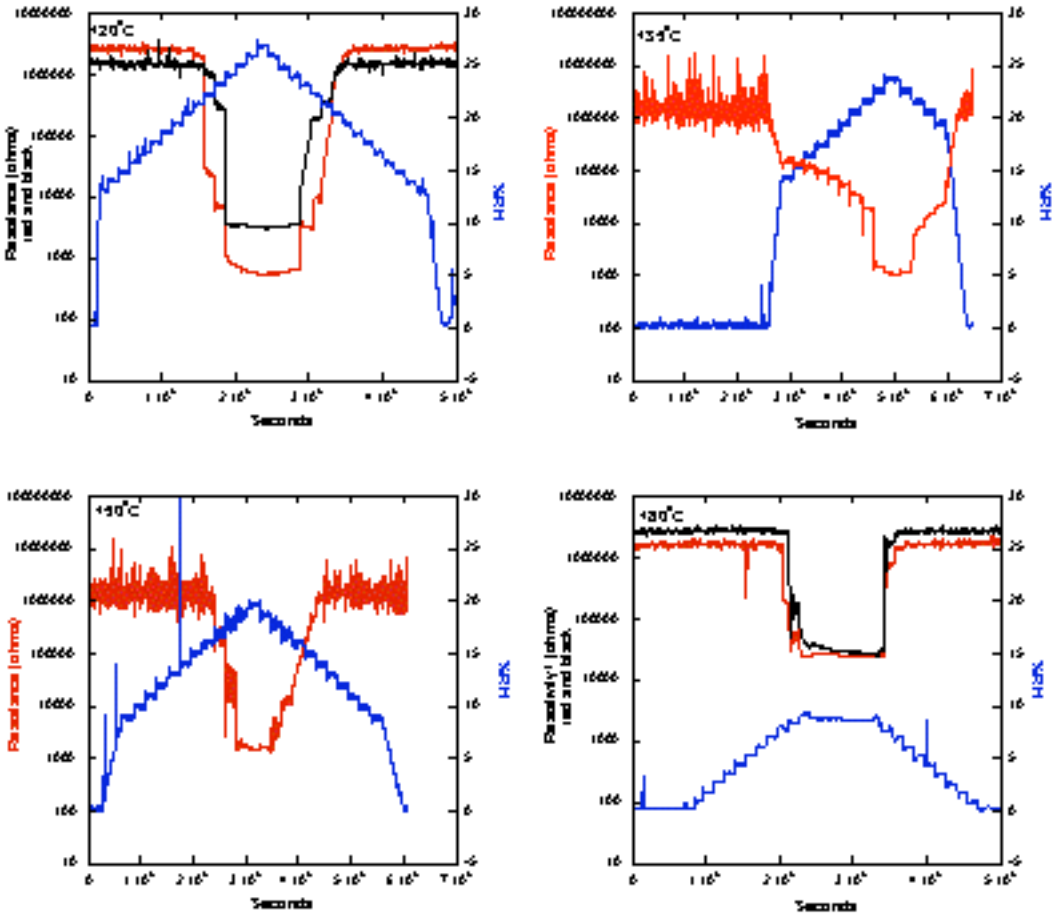

Fig. 7. Results from the measurement of mutual deliquescence/efflorescence relative humidity for $NaNO_3$ + KNO_3 salt mixtures at 120 (top left), 135 (top right), 150 (bottom left), and 180 (bottom right) °C. The mutual deliquescence/efflorescence relative humidity corresponds to a drop/increase in resistance as the salt mixture transforms from a solid to a liquid aqueous solution and from the liquid aqueous solution back to the solid. The RH (percent) probe readings have not been corrected for calibrations with the bi-thermal apparatus at high temperatures, but these corrections are not noticeable to the scale of these plots.

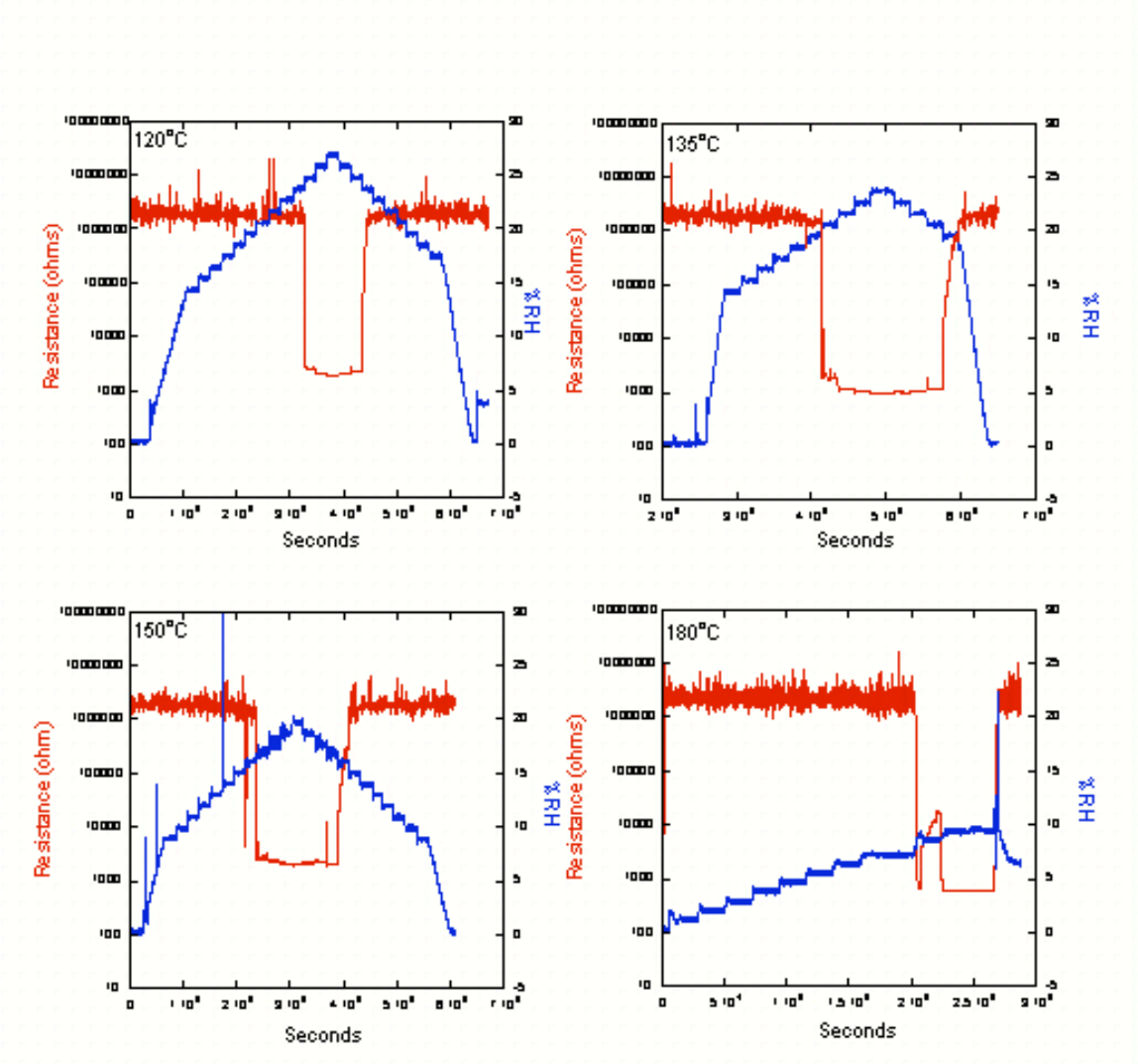

Fig. 8. Results from the measurement of mutual deliquescence/efflorescence relative humidity for NaCl + $NaNO_3$ + KNO_3 salt mixtures at 120 (top left), 135 (top right), 150 (bottom left), and 180 (bottom right) °C. The mutual deliquescence/efflorescence relative humidity corresponds to a drop/increase in the resistance as the salt mixture transforms from a solid to a liquid aqueous solution and from the liquid aqueous solution back to the solid. The RH (percent) probe readings have not been corrected for calibrations with the bi-thermal apparatus at high temperatures, but these corrections are not noticeable to the scale of these plots.

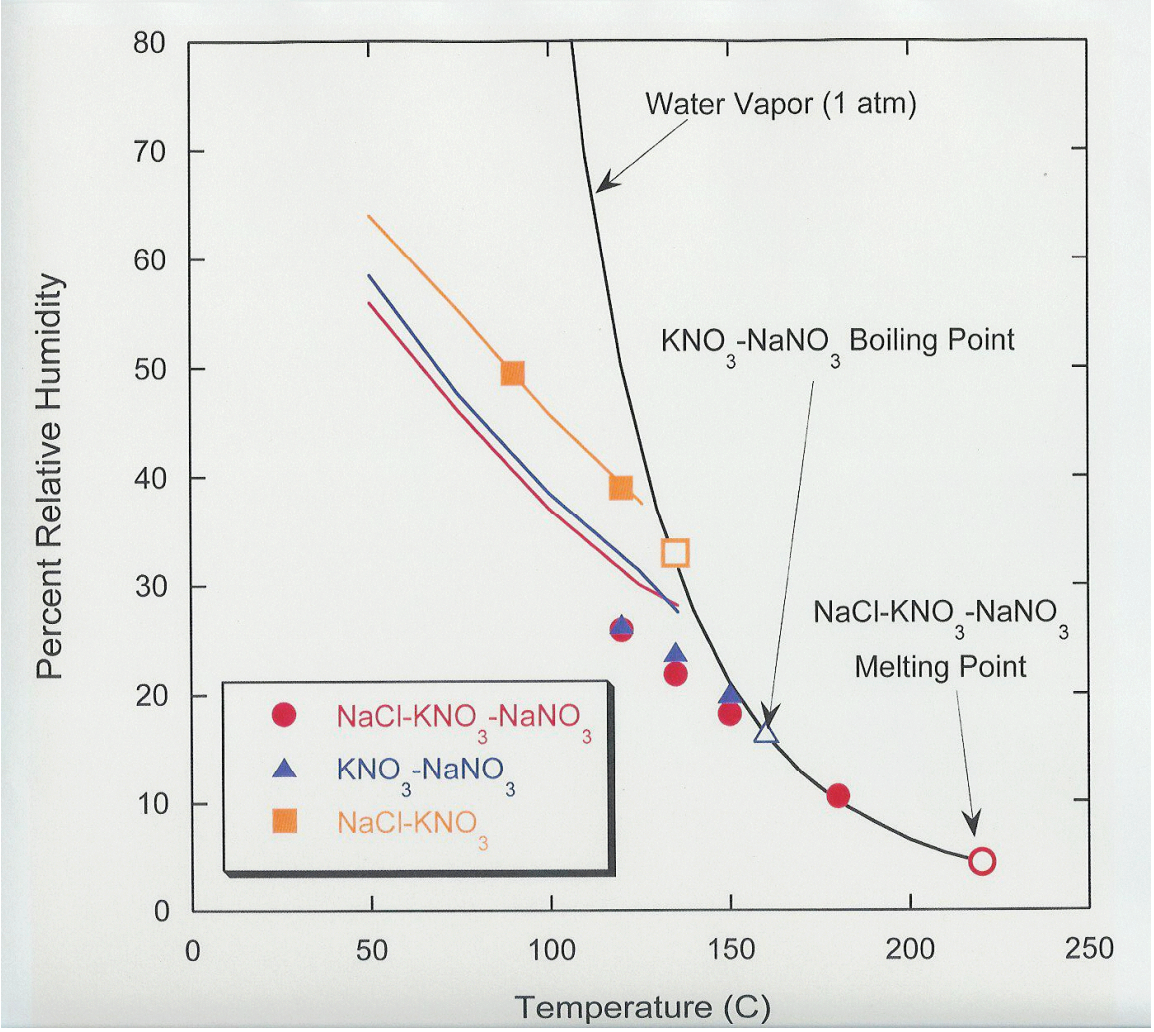

Fig. 9. Comparison of measured and modeled mutual deliquescence relative humidity for NaCl + KNO_3 (Carroll *et al.*[9]), and KNO_3 + $NaNO_3$ and NaCl + KNO_3 + $NaNO_3$ (this study from Table VII) salt mixtures as a function of temperature. Maximum boiling temperatures (Tables I and II) and the melting temperature were determined in this study. The RH (percent) has been corrected at higher temperatures for the calibration of the sensors using the bi-thermal apparatus. The curve labeled "Water Vapor" is that for the relative humidity of water vapor at 1 bar pressure. Closed symbols: directly measured MDRH/MERH; orange and blue open symbols: boiling temperatures; open red circle, melting temperature.